An alternate approach to the ignition regime for inertial confinement fusion

HEDS Seminar

21 January 2021

Steve MacLaren for the PSS Team

This work was performed under the auspices of the U.S. Department of Energy by Lawrence Livermore National Laboratory under contract DE-AC52-07NA27344. Lawrence Livermore National Security, LLC

Lawrence Livermore National Laboratory

A slower, more massive implosion, the pushered single shell (PSS) offers a fundamentally different trajectory towards the ignition threshold

- We describe a threshold that motivates the design the PSS, reaching ignition at lower velocity and temperature
- Using ARC, the ID PSS platform on NIF has demonstrated tunable long-pulse implosions of the kind necessary for low-adiabat compression
- The graded-density profile, successfully fabricated into Be capsules, predicts to mitigate ablation front instability so as to allow good compression at increased confinement

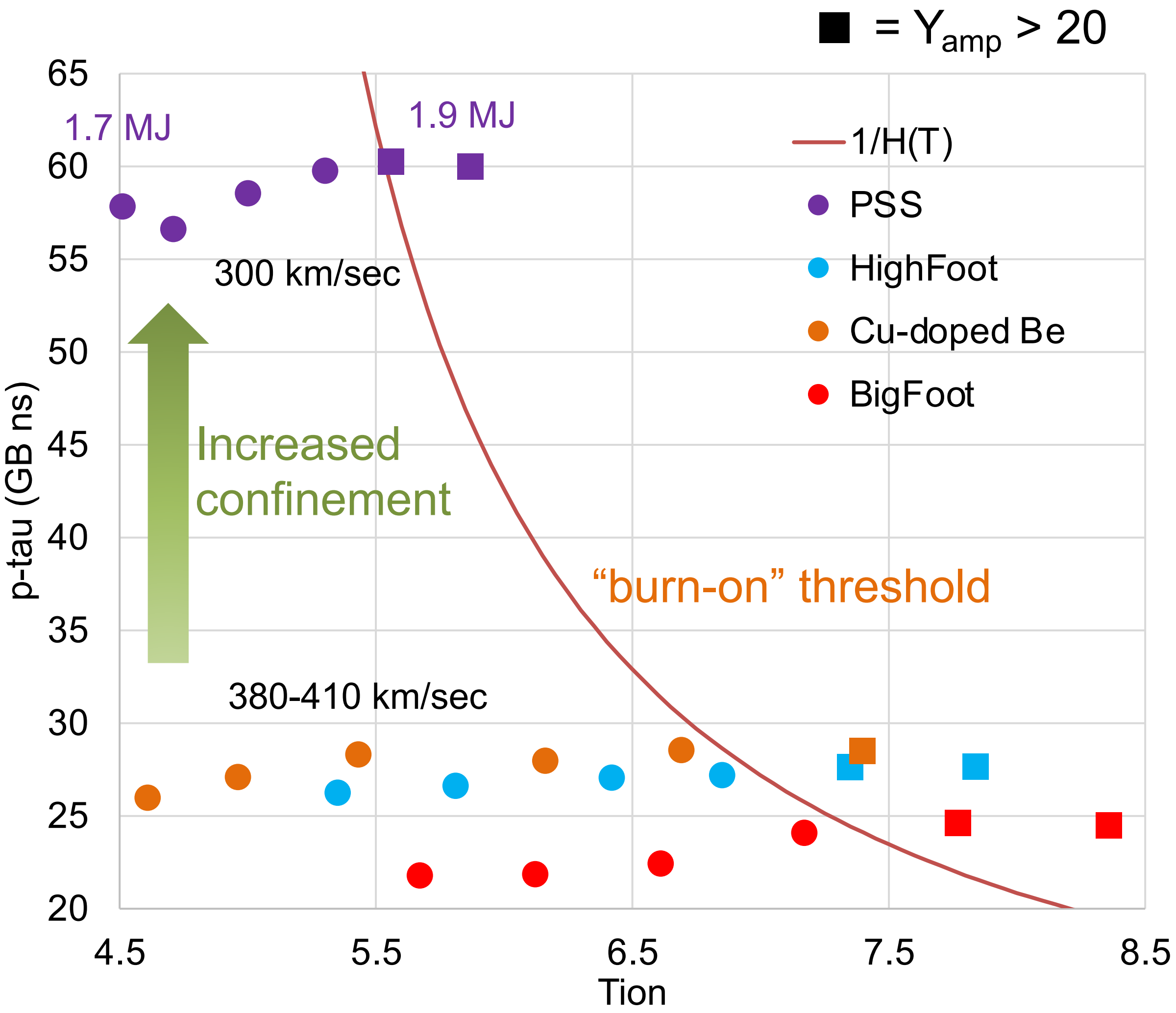

The Pushered Single Shell Team is a collaboration between LLNL and GA

- LLNL
  - Eddie Dewald
  - David Martinez
  - Darwin Ho
  - Bob Tipton
  - Corie Horwood
  - Jessie Pino
  - Chris Young
  - Justin Buscho
  - Elvin Monzon
  - Greg Mellos
  - Allison Engwall
  - Scott Vonhof

- GA
  - Hongwei Xu
  - Jon Bae
  - Casey Kong
  - Neil Rice
  - Kevin Sequoia
  - Haibo Huang

Outline

- Theoretical description of the ignition regime
- Description of the pushered single shell (PSS) design and capsule fabrication
- PSS results on the NIF
- Detailed analysis of PSS stability

The ignition condition can be described as a race between the rate of alpha-heating and the disassembly rate

- “The alpha heating will exceed the losses for some time after the start of expansion. The duration over which this occurs will depend on the temperature achieved before the start of expansion.”[1]
- $\Delta t_{bootstrap}$ is the characteristic time over which the heating rate is evaluated
- The disassembly rate will be determined by the hydro characteristics of the burn-off implosion

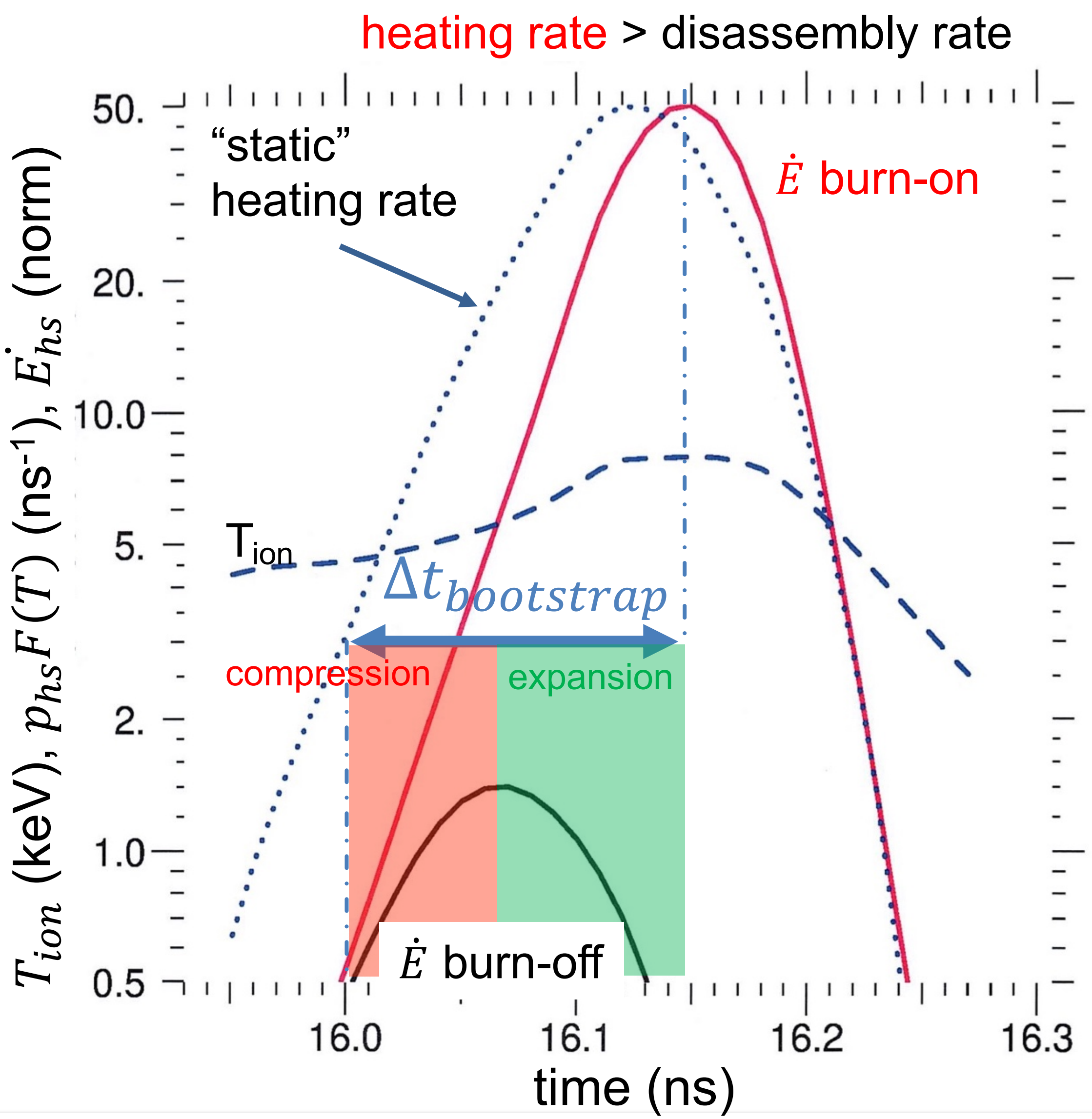

[1]Lindl et al, PoP **25**,122704, 2018

Heating rate: from the hot-spot power balance

$$C_{DT}\frac{dT}{dt} = f_\alpha Q_\alpha - f_B Q_B - Q_e - \frac{1}{m} p \frac{dV}{dt} - Q_{other}$$

Dynamic hot spot power balance

$$\frac{dE_{hs}}{dt} = C_{DT} T \frac{dm}{dt} + C_{DT} m \frac{dT}{dt}$$

Hot spot thermodynamics
heat capacity

$$\frac{dm}{dt} = \frac{m}{C_{DT} T}[(1 - f_\alpha)Q_\alpha + Q_e]$$

Mass accretion assumptions

Heating rate: from the hot-spot power balance

$$\frac{dE_{hs}}{dt} = C_{DT}T\frac{dm}{dt} + C_{DT}m\frac{dT}{dt}$$

Hot spot thermodynamics heat capacity

$$C_{DT}\frac{dT}{dt} = f_\alpha Q_\alpha - f_B Q_B - Q_e - \frac{1}{m}p\frac{dV}{dt} - Q_{other}$$

Dynamic hot spot power balance

Valid only for cryo fuel layer

$$\frac{dm}{dt} = \frac{m}{C_{DT}T}\left[(1 - f_\alpha)Q_\alpha + Q_e\right]$$

Mass accretion assumptions

Heating rate: from the hot-spot power balance

$$E_{hs} = mC_{DT}T$$

$$\frac{dE_{hs}}{dt} = C_{DT}T\frac{dm}{dt} + C_{DT}m\frac{dT}{dt}$$

Hot spot thermodynamics heat capacity

$$C_{DT}\frac{dT}{dt} = f_\alpha Q_\alpha - f_B Q_B - Q_e - \frac{1}{m}p\frac{dV}{dt} - Q_{other}$$

Dynamic hot spot power balance

Valid only for cryo fuel layer

$$\frac{dm}{dt} = \frac{m}{C_{DT}T}\left[(1-f_\alpha)Q_\alpha + Q_e\right]$$

Mass accretion assumptions

Combine these to get the net heating rate:

$$\frac{\dot{E}_{hs}}{E_{hs}} = \frac{Q_\alpha - f_B Q_B}{C_{DT}T} - \frac{p}{E_{hs}}\frac{dV}{dt} = pF(T) - \frac{p}{E_{hs}}\frac{dV}{dt} \quad (Q_{other} \to 0)$$

$pF(T)$ is the "static" heating rate

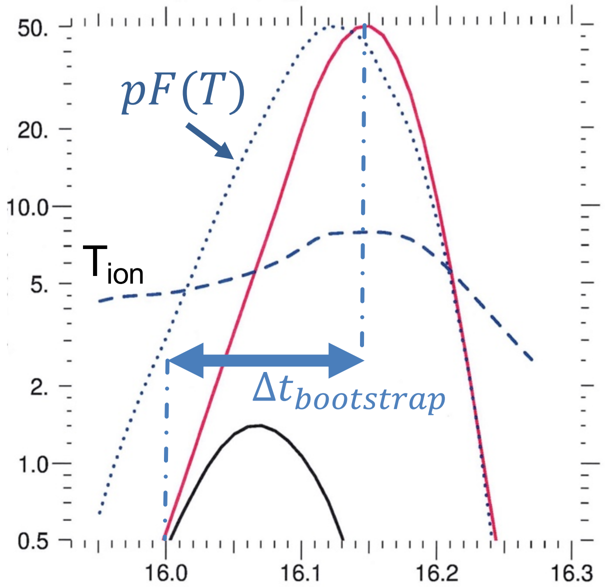

Fortunately, the average heating rate over this critical time has already been calculated[1]:

$$\langle pF(T)\rangle = \frac{\int_0^{t_m} pF(T)dt}{\Delta t_{bootstrap}} = \frac{pH(T_0)\sqrt{\frac{T}{\ddot{T}}}}{\Delta t_{bootstrap}} \cong pH(T_0)$$

[1]Hurricane et al., PoP **26**, 052704 (2019)

Using a fit to the Bosch and Hale DT reactivity accurate between 2<T<10 keV, we get an algebraic form for the temperature in the heating rate

F(T) depends on $\langle \sigma v \rangle (T)$ through Q_α, so Hurricane[1] fits Bosch and Hale:

$$F(T) \approx [4.7 + 11 f_B + (0.4 + 0.86 f_B) T] \ln\left(\frac{T}{4.3 f_B^{0.3}}\right) \times 10^8 \, \frac{cm^2}{GJ \cdot s}$$

for $\langle \sigma v \rangle (T)$ 2<T<10 keV

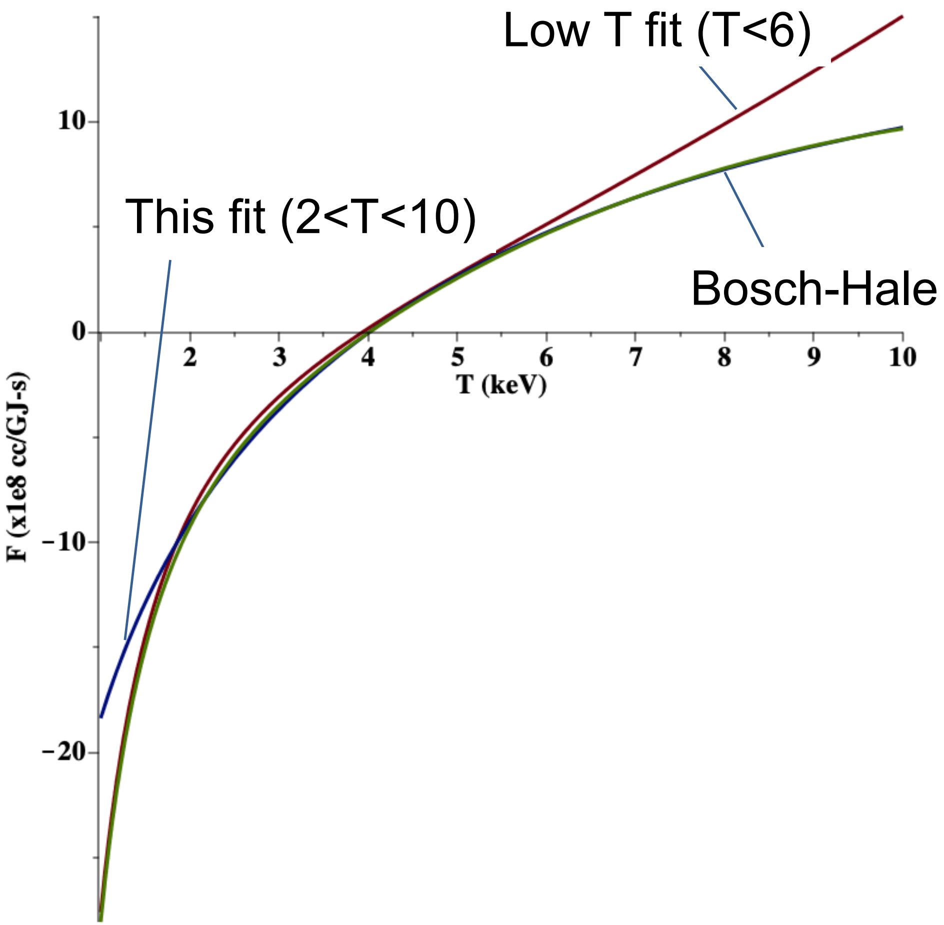

Average heating rate: integration over the "bootstrap" time

$$\langle pF(T) \rangle = \frac{\int_0^{t_m} pF(T)dt}{\Delta t_{bootstrap}} \cong pH(T_0)$$

$$H_s(T_{max}) = \frac{\sqrt{\pi} F(T_{max})}{\sqrt{\frac{2\gamma}{\gamma - 1} + \frac{2T_{max}}{F(T_{max})} \left.\frac{\partial F}{\partial T}\right|_{T_{max}}}}$$

From method of "steepest decent"

Then,

$$H_s(T_{max}) \approx \frac{\sqrt{\pi} 10^{-2} [a(f_B) + b(f_B) T_{max}] \ln\left(\frac{T_{max}}{T_{ign}}\right)}{\sqrt{\frac{2\gamma}{\gamma-1} + \frac{2T_{max}}{[a(f_B)+b(f_B)T_{max}] \ln\left(\frac{T_{max}}{T_{ign}}\right)} \left[\frac{a(f_B)+b(f_B)T_{max}}{T_{max}} + b(f_B) \ln\left(\frac{T_{max}}{T_{ign}}\right)\right]}}$$

$$T_{ign} = 4.3 f_B^{0.3}$$

[1]Hurricane et al., Phys. Plasmas, accepted 8 Jan 2021

Disassembly rate: from the definition of τ_{conf} terms of stagnated mass

Expand the pdV term about minimum volume:

- $$\frac{p}{E_{hs}}\frac{dV}{dt} = \frac{2}{3V}\frac{d^2V}{dt^2}(t - t_{min}) = \frac{2}{3V}\left[\int (R^2\ddot{R} + 2R\dot{R})d\Omega\right](t - t_{min})$$

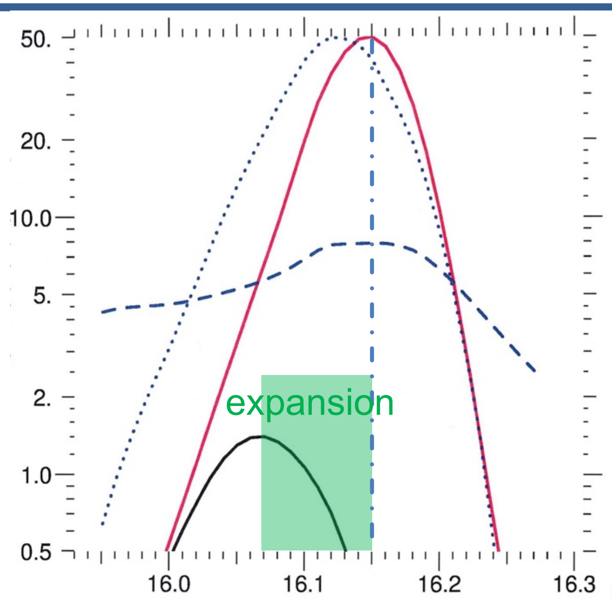

[1]Springer et al., Nuclear Fusion **59**, 032009 (2018)

Disassembly rate: from the definition of τ_{conf} terms of stagnated mass

Expand the pdV term about minimum volume:

- $$\frac{p}{E_{hs}}\frac{dV}{dt} = \frac{2}{3V}\frac{d^2V}{dt^2}(t - t_{min}) = \frac{2}{3V}\left[\int (R^2\ddot{R} + 2R\dot{R})d\Omega\right](t - t_{min})$$

residual 3D shell velocity

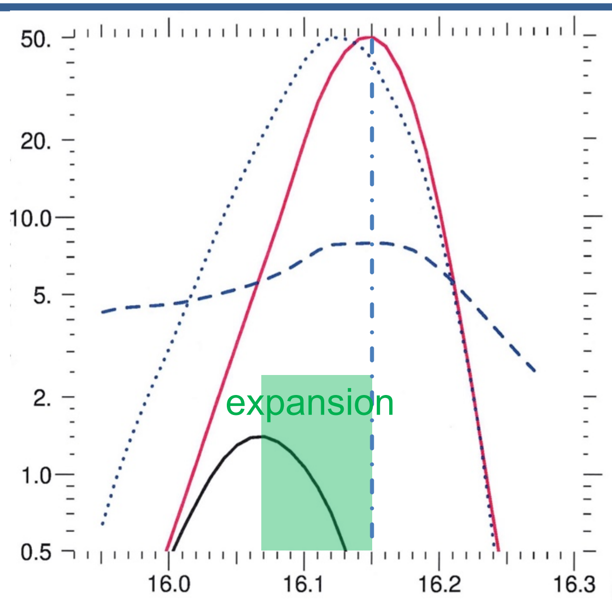

[1]Springer et al., Nuclear Fusion **59**, 032009 (2018)

Disassembly rate: from the definition of τ_{conf} terms of stagnated mass

Expand the pdV term about minimum volume:

- $$\frac{p}{E_{hs}}\frac{dV}{dt} = \frac{2}{3V}\frac{d^2V}{dt^2}(t - t_{min}) = \frac{2}{3V}\left[\int (R^2\ddot{R} + 2R\dot{R})d\Omega\right](t - t_{min})$$

residual 3D shell velocity

- Newton's law for the force exerted by the ΔP across the stagnation shock at minimum volume (e.g. Springer et al[1].): $$\ddot{R}_{hs} = \frac{p_{hs}}{M_{stag}}4\pi R_{hs}^2$$

- Identifying $2\times(t - t_{min}) = \tau_{conf} \approx \sqrt{\frac{M_{stag}}{p_{hs}4\pi R_{hs}}}$ {Betti et al., PoP 17, 058102 (2010)}

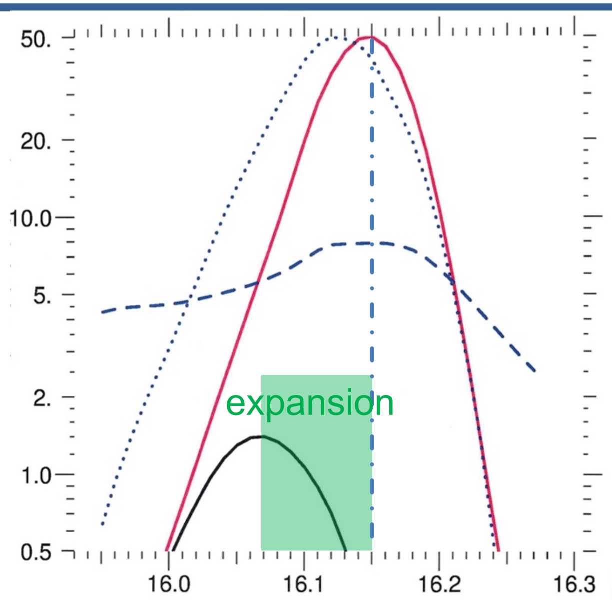

[1]Springer et al., Nuclear Fusion **59**, 032009 (2018)

Disassembly rate: from the definition of τ_{conf} terms of stagnated mass

Expand the pdV term about minimum volume:

$$\frac{p}{E_{hs}}\frac{dV}{dt} = \frac{2}{3V}\frac{d^2V}{dt^2}(t-t_{min}) = \frac{2}{3V}\left[\int (R^2\ddot{R} + 2R\dot{R})d\Omega\right](t-t_{min})$$

residual 3D shell velocity

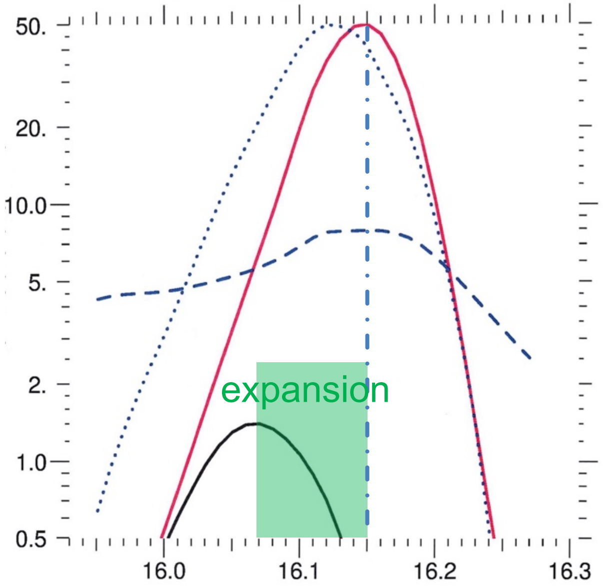

Newton's law for the force exerted by the ΔP across the stagnation shock at minimum volume (e.g. Springer et al[1].): $\ddot{R}_{hs} = \frac{p_{hs}}{M_{stag}} 4\pi R_{hs}^2$

Identifying $2\times(t-t_{min}) = \tau_{conf} \approx \sqrt{\frac{M_{stag}}{p_{hs}4\pi R_{hs}}}$ {Betti et al., PoP 17, 058102 (2010)}

$$\frac{\dot{E}_{hs}}{E_{hs}} = p_{hs}H(T_0) - \frac{2}{3V}4\pi R^2\ddot{R}(t-t_{min}) = p_{hs}H(T_0) - \left[\frac{p_{hs}4\pi R_{hs}}{M_{stag}}\right]\tau_{conf} = p_{hs}H(T_0) - \frac{1}{\tau_{conf}}$$

Require that the net heating rate near minimum volume be positive:

$$p_{hs}H(T_0) > \sqrt{\frac{p_{hs}4\pi R_{hs}}{M_{stag}}} \approx \frac{1}{\tau_{conf}}$$

HS heating rate > Disassembly rate

P-τ goes like $\sqrt{\frac{p_{hs}M_{stag}}{R_{hs}}}$

[1]Springer et al., Nuclear Fusion **59**, 032009 (2018)

By explicitly including the competition of rates, the burn-on criteria better identifies the onset of significant yield amplification

$$p_{hs} H(T_0) > \sqrt{\frac{p_{hs} 4\pi R_{hs}}{M_{stag}}} \quad \rightarrow \quad p_{hs}\tau_{conf} > \frac{1}{H(T_0)}$$

HS heating rate > Disassembly rate

Generalized Lawson Criterion (burn-off)

Ignition metric using "burn-on" peak temperature

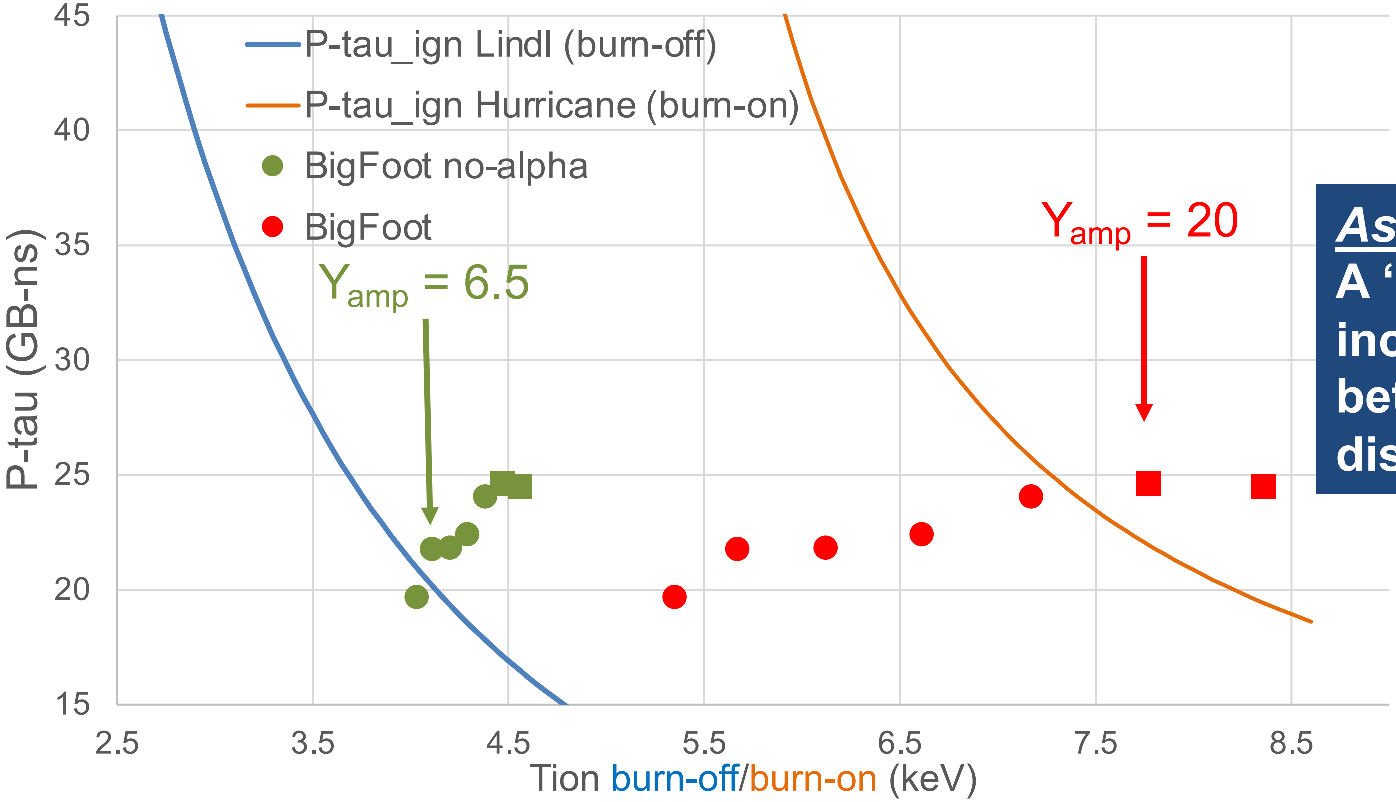

Assertion:
A "burn-on" metric, with the *temperature feedback* incorporated in $H(T_0)$, better captures the "race" between the competing effects of heating and disassembly during the "bootstrapping" period

Comparison of $P\tau_{ign}$ from:
Lindl et al., PoP **25**, 122704 (2018) eq 18
Hurricane et al., PoP accepted 2021

Outline

- Theoretical description of the ignition regime
- Description of the pushered single shell (PSS) design and capsule fabrication
- PSS results on the NIF
- Detailed analysis of PSS stability

To increase mass at stagnation, the Pushered Single Shell concept uses a graded density inner ablator layer

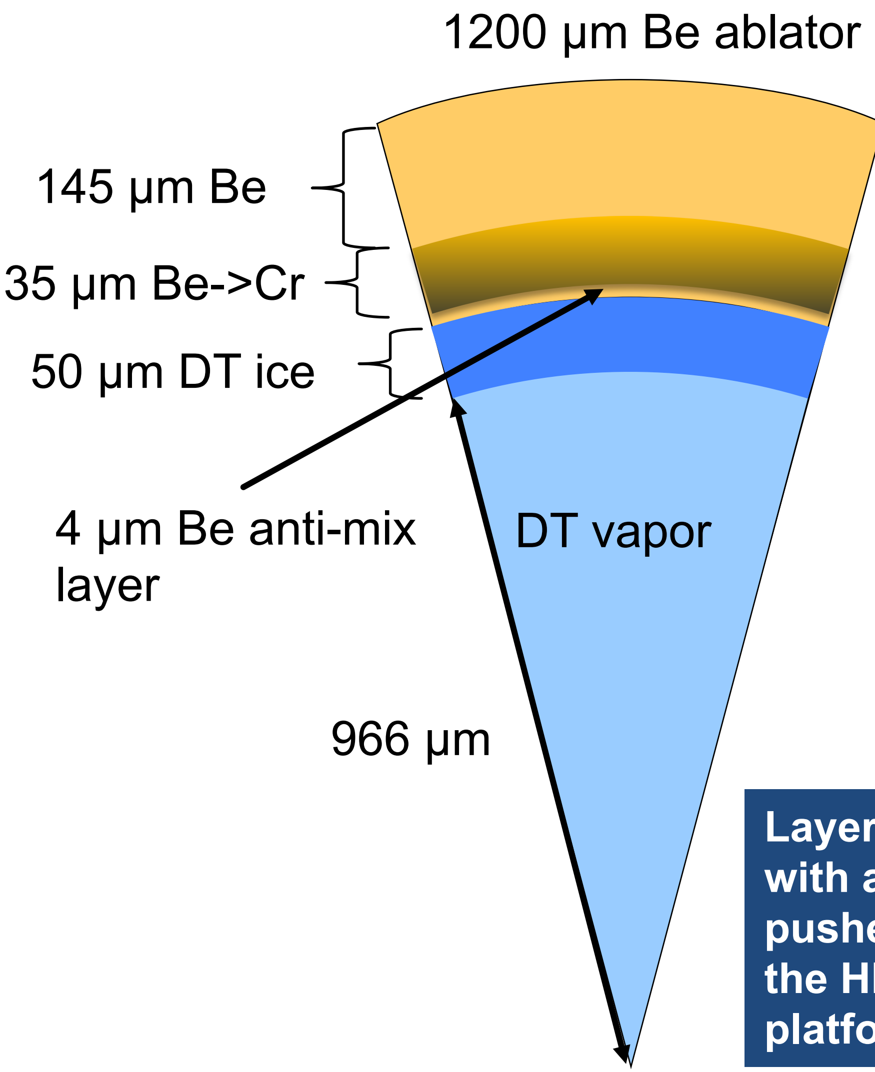

Layered design is optimized with a lighter, narrower peak pusher density region than the HED metal-gas mix platform

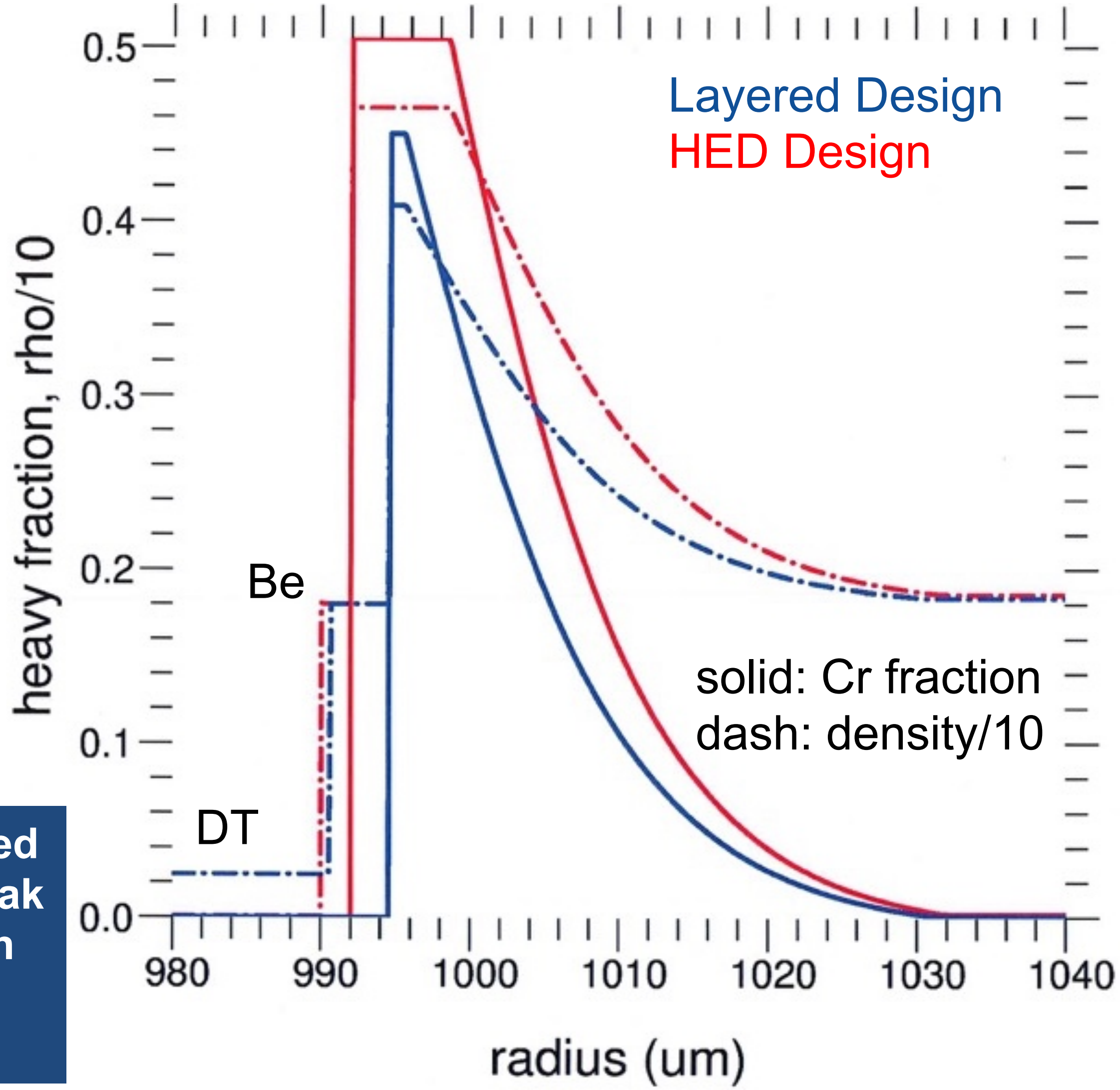

Pushered Single Shells for the laboratory are not a new idea

- Tahir and Long, *Nuclear Instruments and Methods in Physics Research, Section A* 278.1 (1989): 118-122.
  - Pb tamper and radiation shield
- Basko, Nuclear Fusion **30**, 12 (1990): 2443-52.
  - Au tamper
- Lackner, Colgate et al., "Equilibrium ignition for ICF capsules." *AIP Conference Proceedings*. Vol. 318. No. 1. AIP, 1994
  - Equilibrium burn in PSS is much less sensitive to shell adiabat
- Wilson et al., *Fusion Technology* 38.1 (2000): 16-21.
  - Cryogenic DT layered beryllium PSS with 6 μm W layer
- Milovich et al., Phys Plasmas **11**, 1552 (2004), Hu et al., Phys. Rev. E **100** 063204 (2019)
  - Graded metal shell for double shell
- Perkins et al., 53rd DPP (2011APS..DPPUO6002P), Ho et al., Anomalous Absorption 2018
  - Incorporates graded Be-high Z shell into PSS NIF design

General Atomics has demonstrated the ability to deliver smooth, high quality graded Cr->Be shells for PSS experiments

- GA's demonstration of blending Cr with Be in capsule coatings presented the opportunity for a viable PSS implosion platform on NIF

- BeCr capsules in FY21 NIF targets represent 2+ years of fabrication & production technology R&D
  - — Most of which can be applied to current R&D process for BeMo

- PSS team continues to meet every 1-2 weeks with GA collaborators

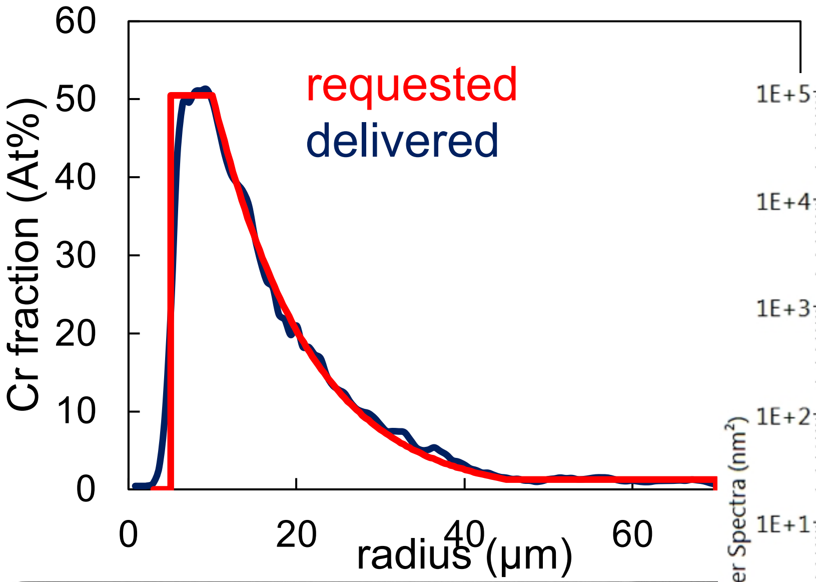

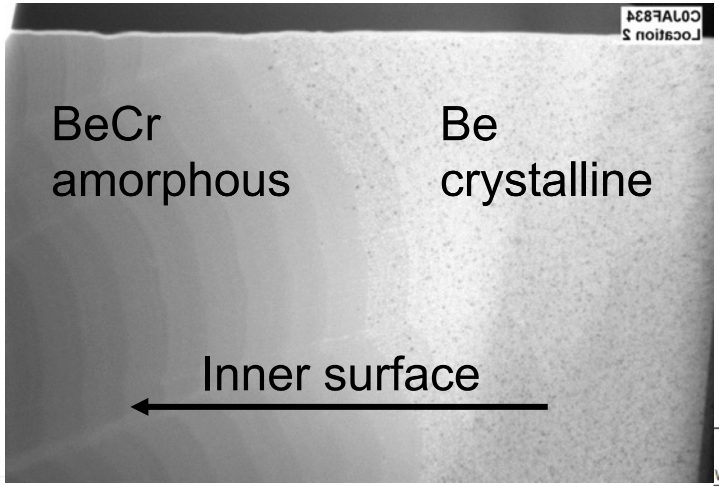

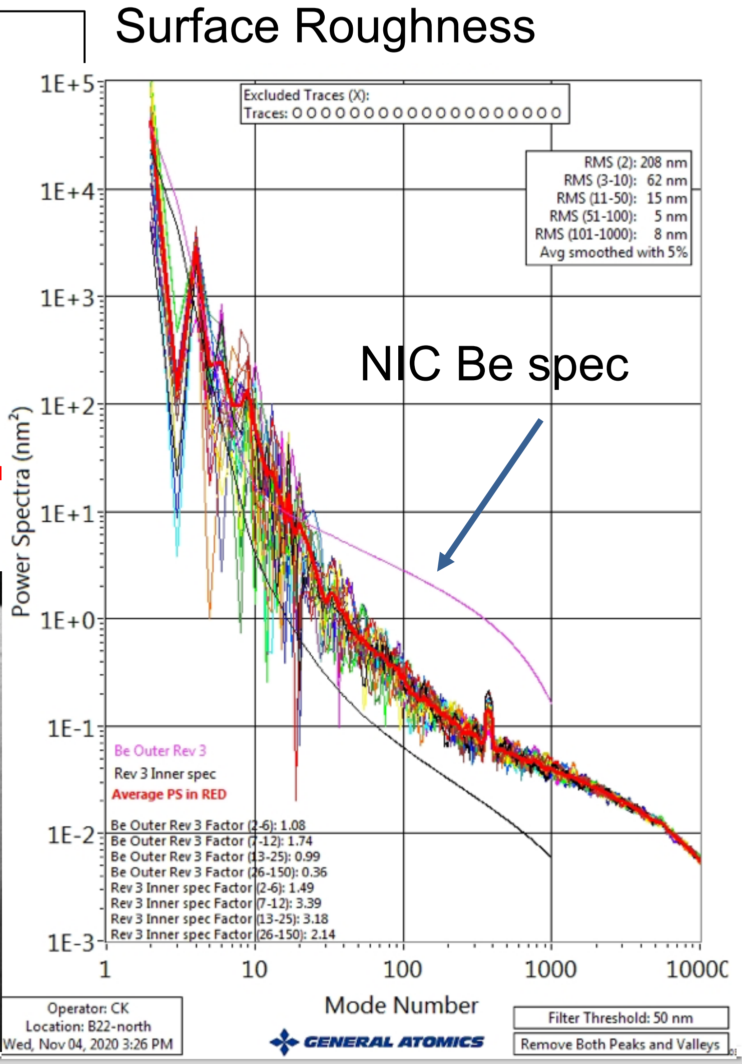

Comparison with the “Big Foot” implosion illustrates effect of M_{stag} on τ_{conf}

$$\tau_{conf} \approx \sqrt{\frac{M_{stag}}{p_{hs} 4\pi R_{hs}}}$$

2.4X 2.2X

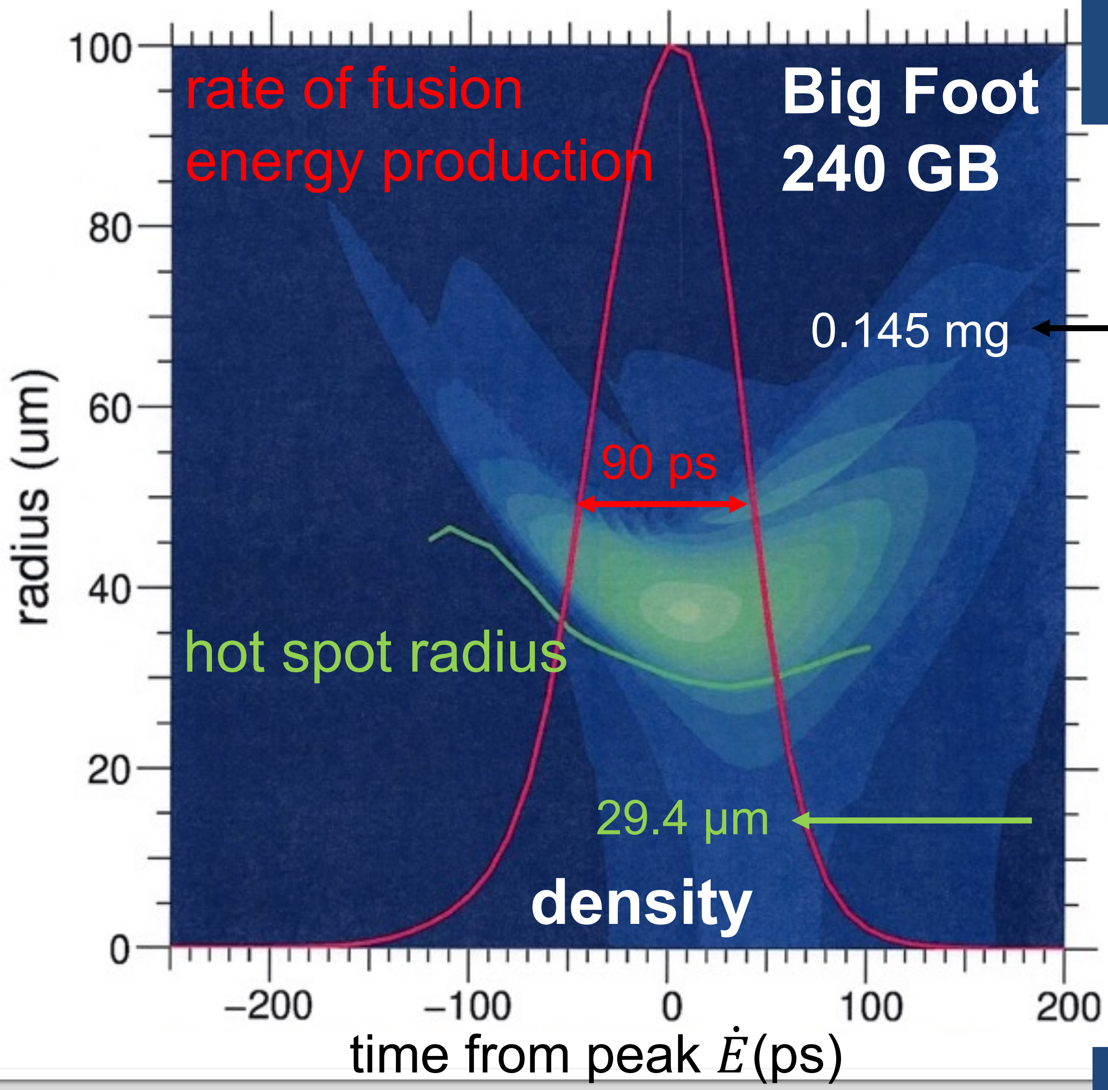

stagnated mass

minimum radius

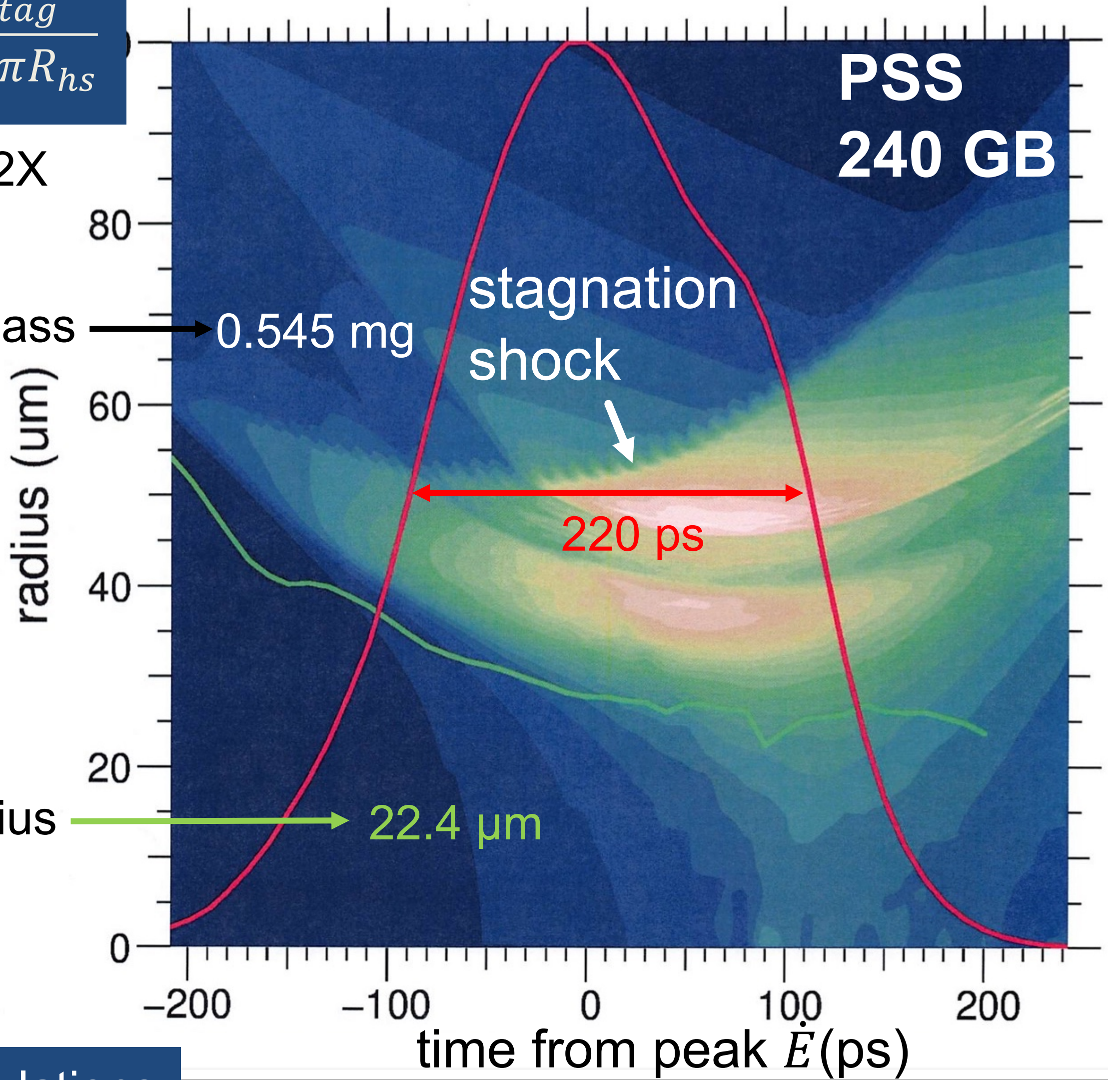

1D ”no-a” simulations

1D simulations are used to validate the threshold theory (through Y_{amp}) and highlight the difference in approach taken by the PSS

Heating rate > disassembly rate $\Rightarrow p_{hs}\,\tau_{conf} H(T_0) > 1$

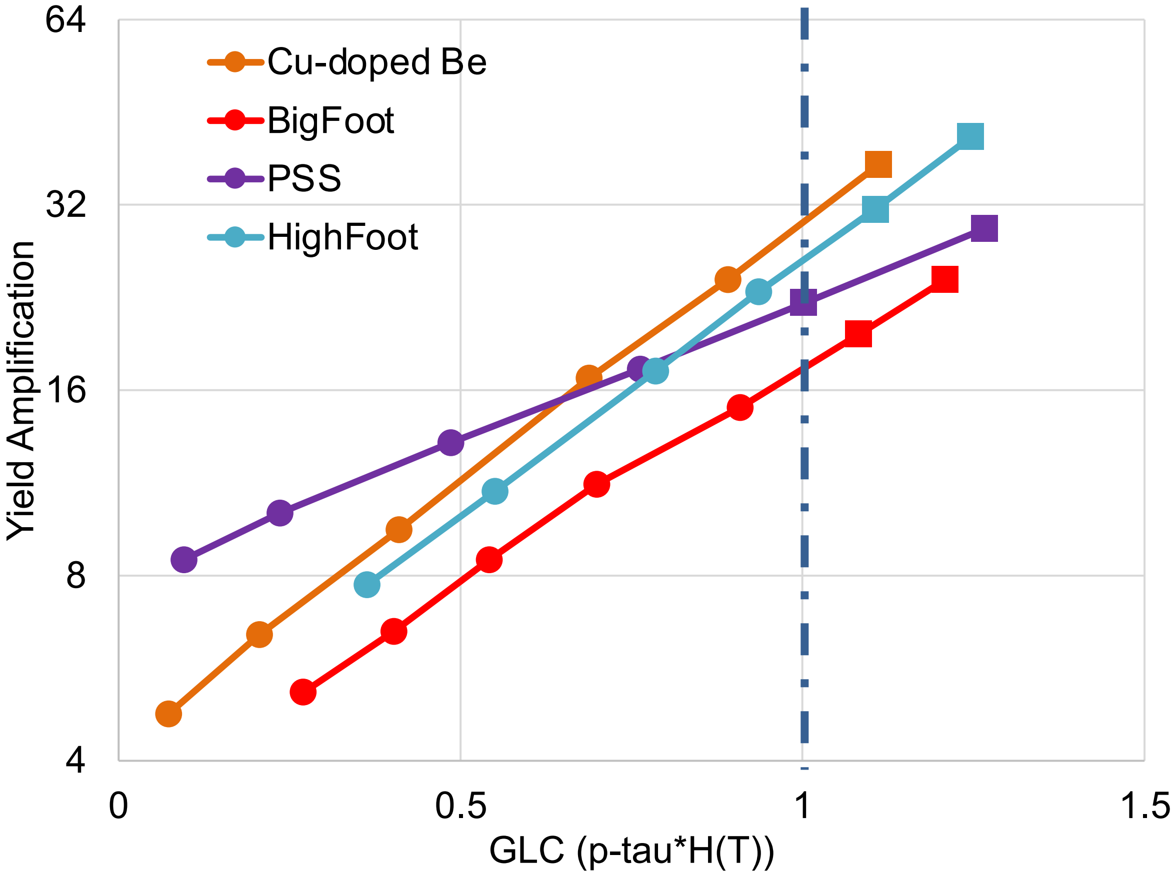

GLC>1: Y_{amp} 20~30 for a broad class of implosions

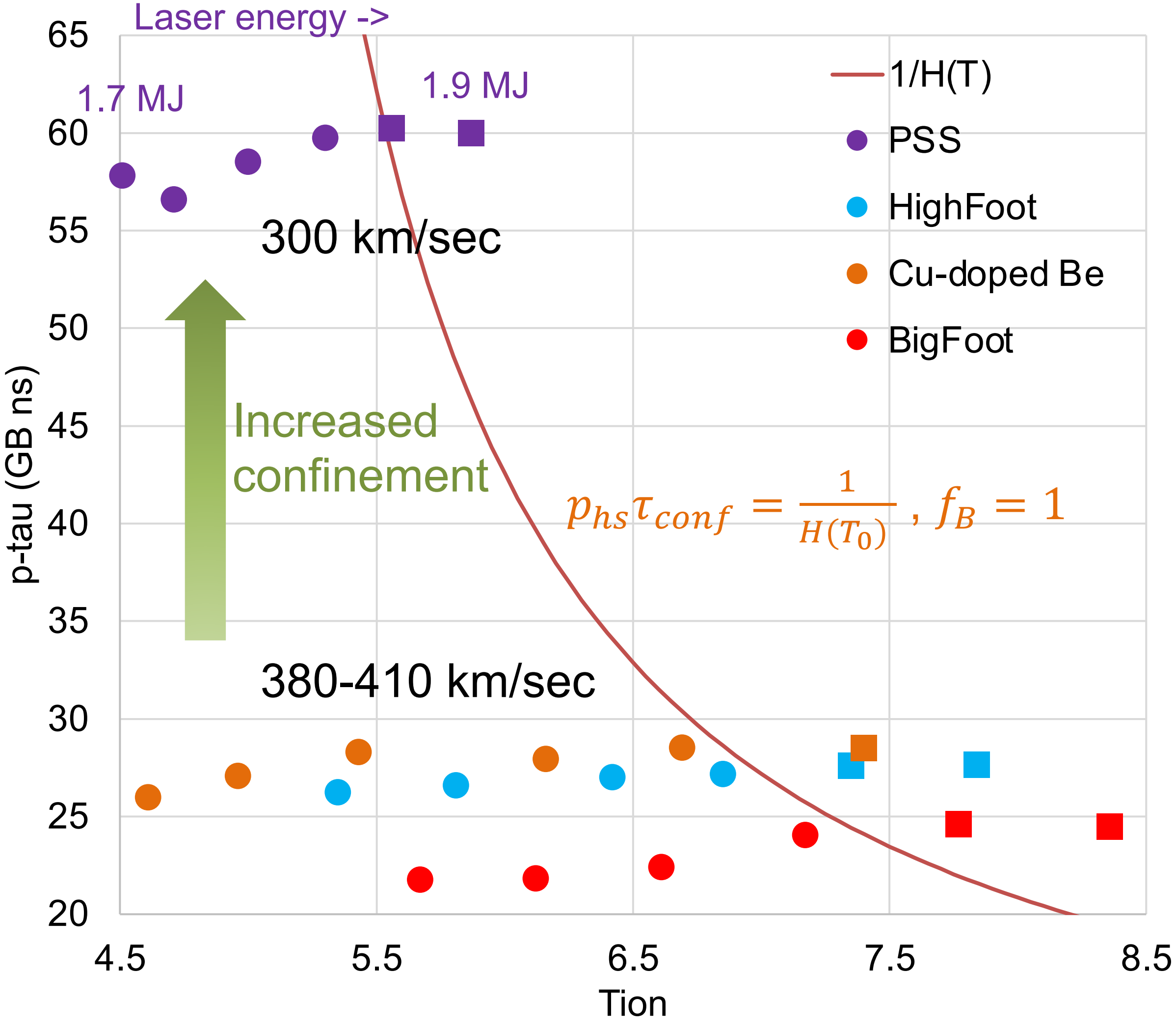

Outline

- Theoretical description of the ignition regime
- Description of the pushered single shell (PSS) design and capsule fabrication
- PSS results on the NIF
- Detailed analysis of PSS stability

Configuration-managed LASNEX simulations are used to model the interaction of the laser pulse with the hohlraum

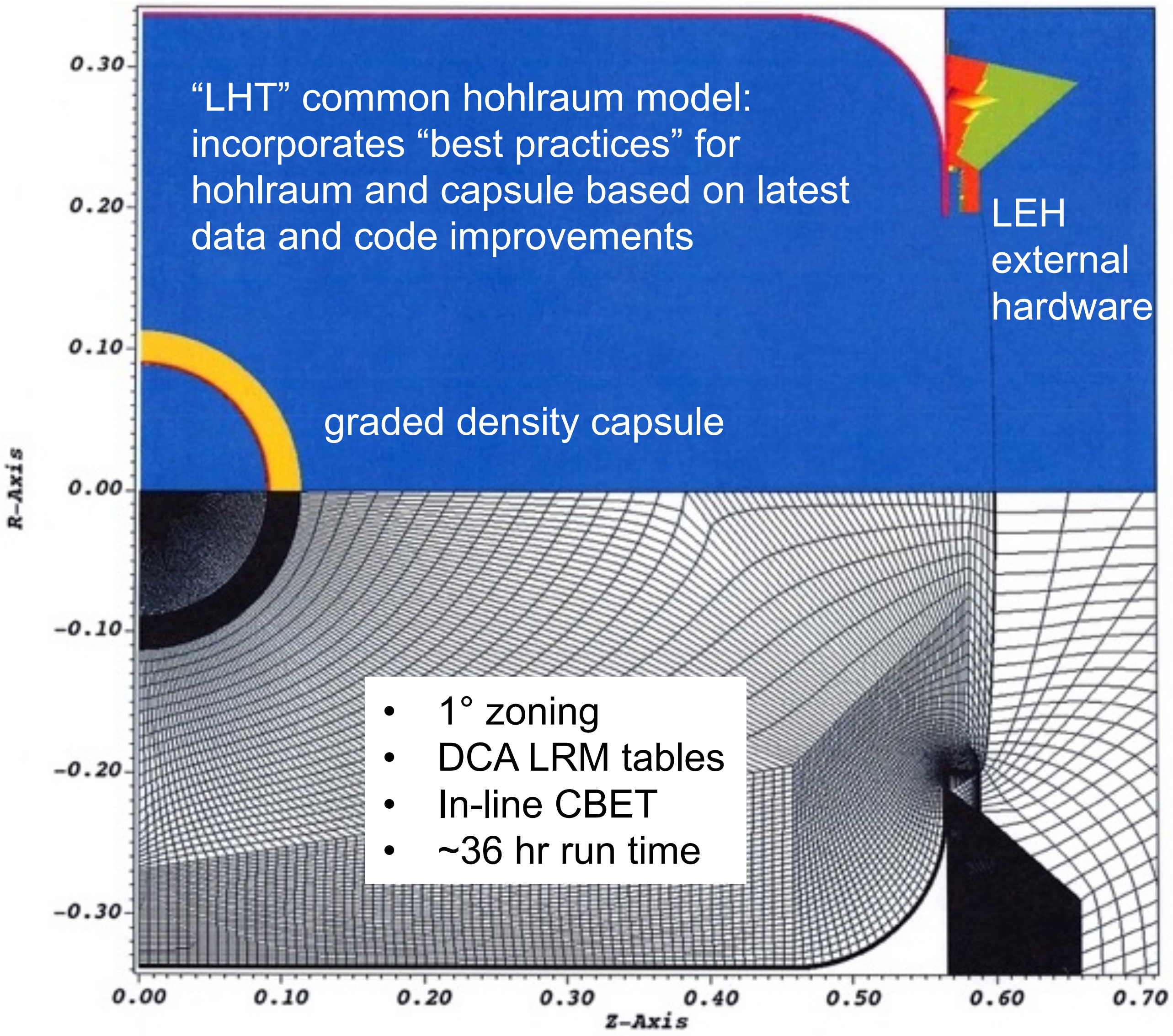

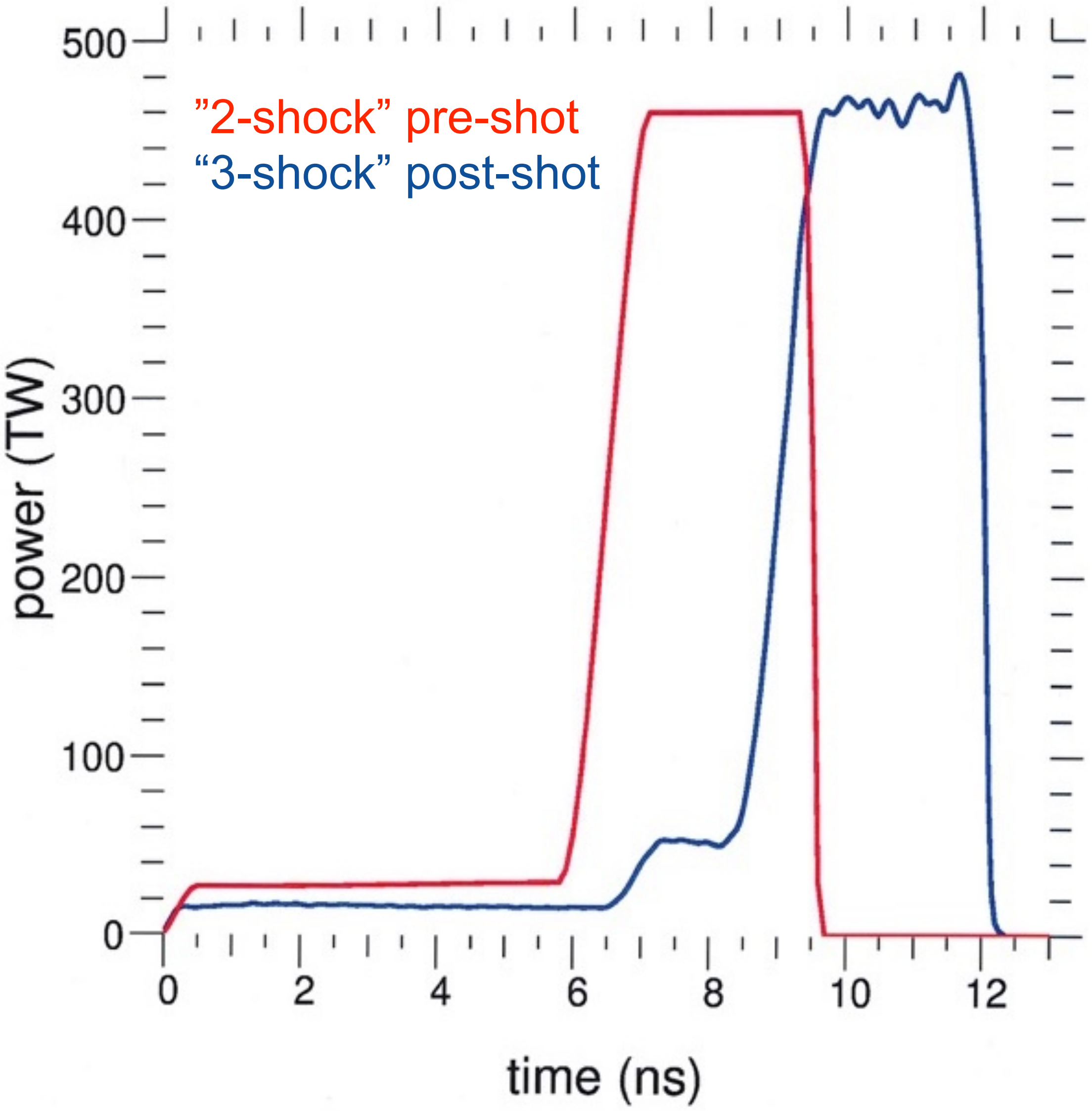

Integrated hohlraum simulations calculate the radiation intensity, spectrum and symmetry incident on the capsule

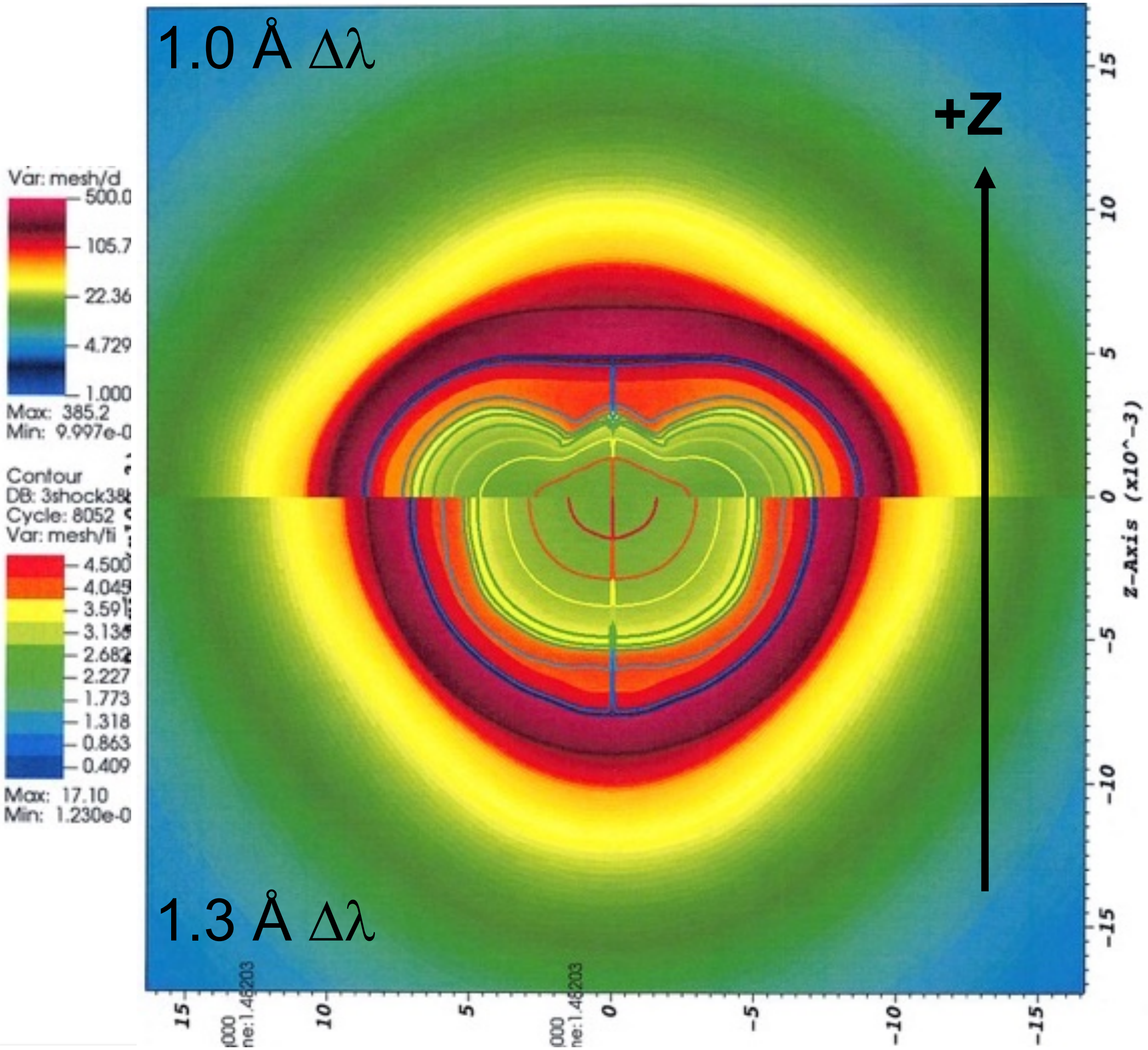

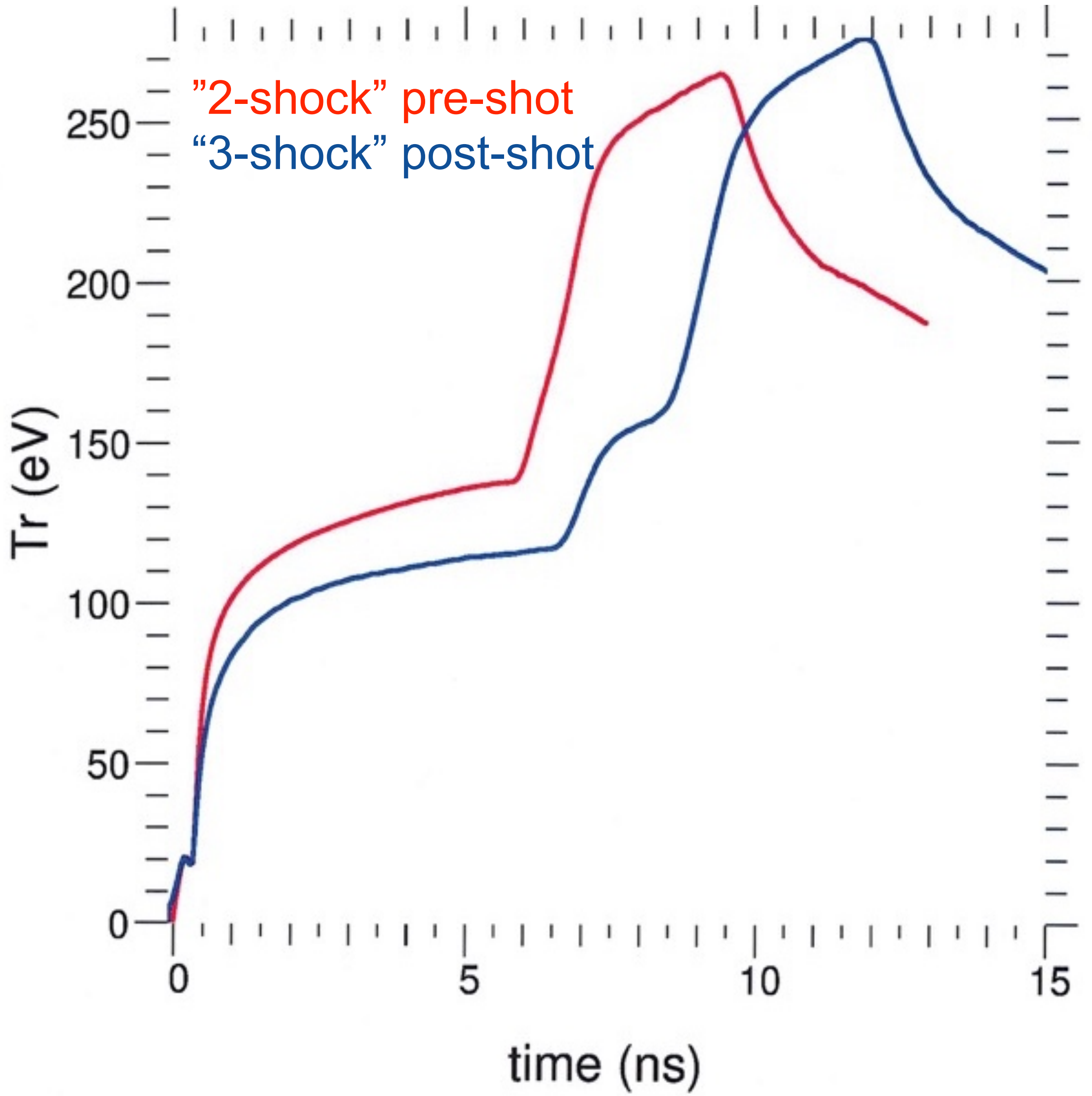

Indirect Drive NIF implosions rely on imaging platforms to tune symmetry

“2D ConA”

N160707-002

Fe area backlighter

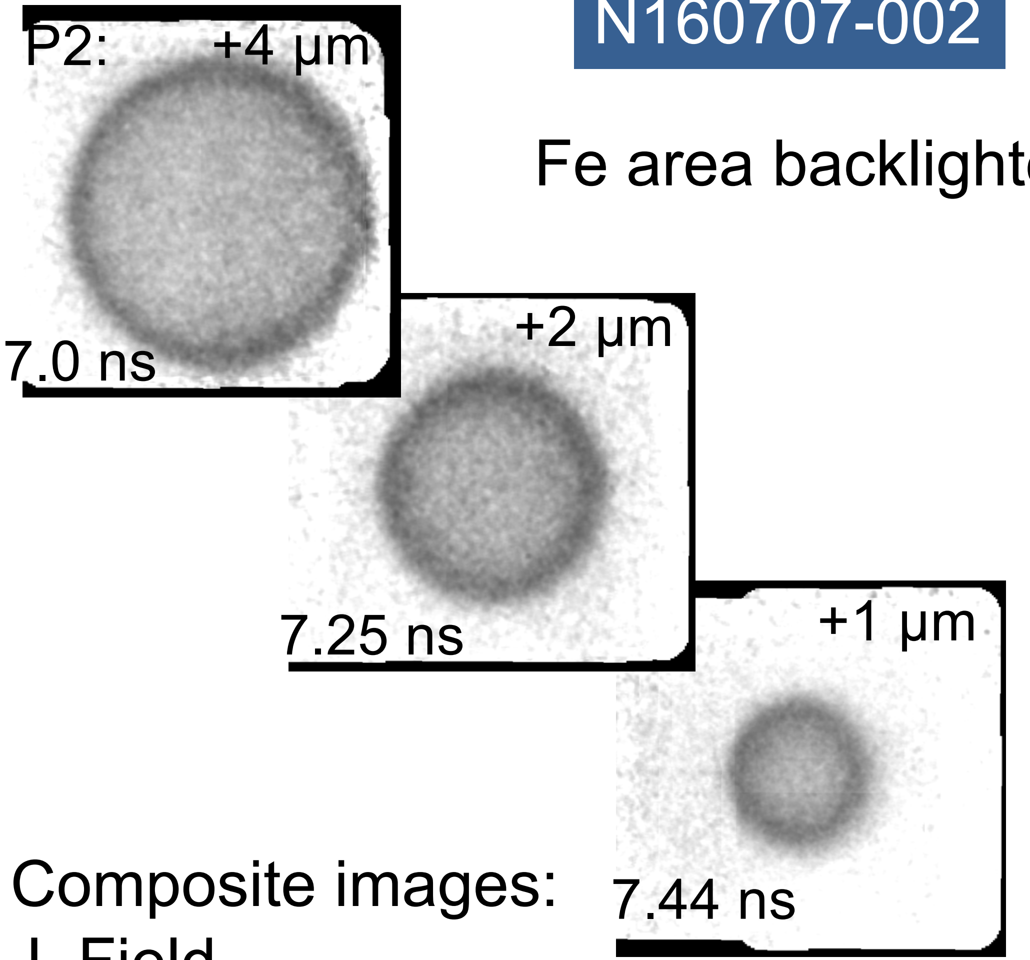

Composite images:
J. Field

“Symcap”

N160721-001

X-ray self emission

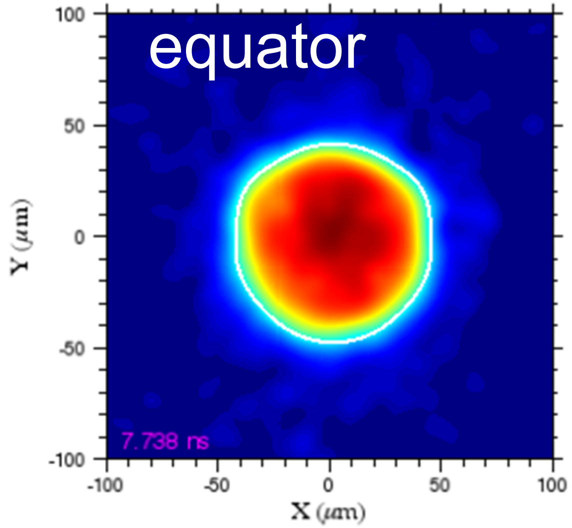

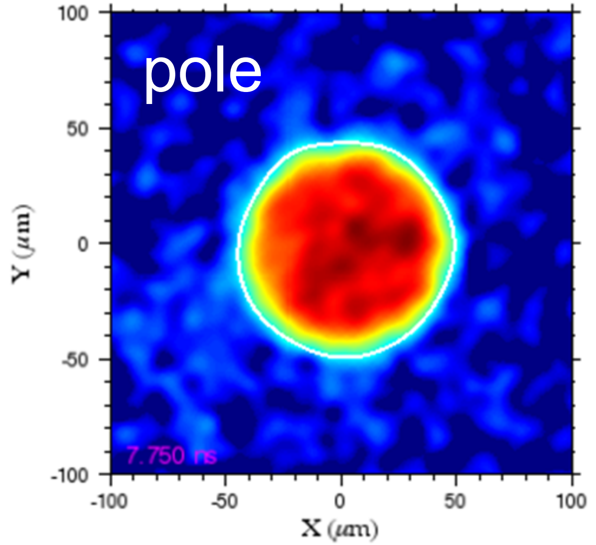

R. Benedetti

PSS capsules require a hard x-ray spectrum to radiograph the inflight shell

Be/Cr "HED" PSS

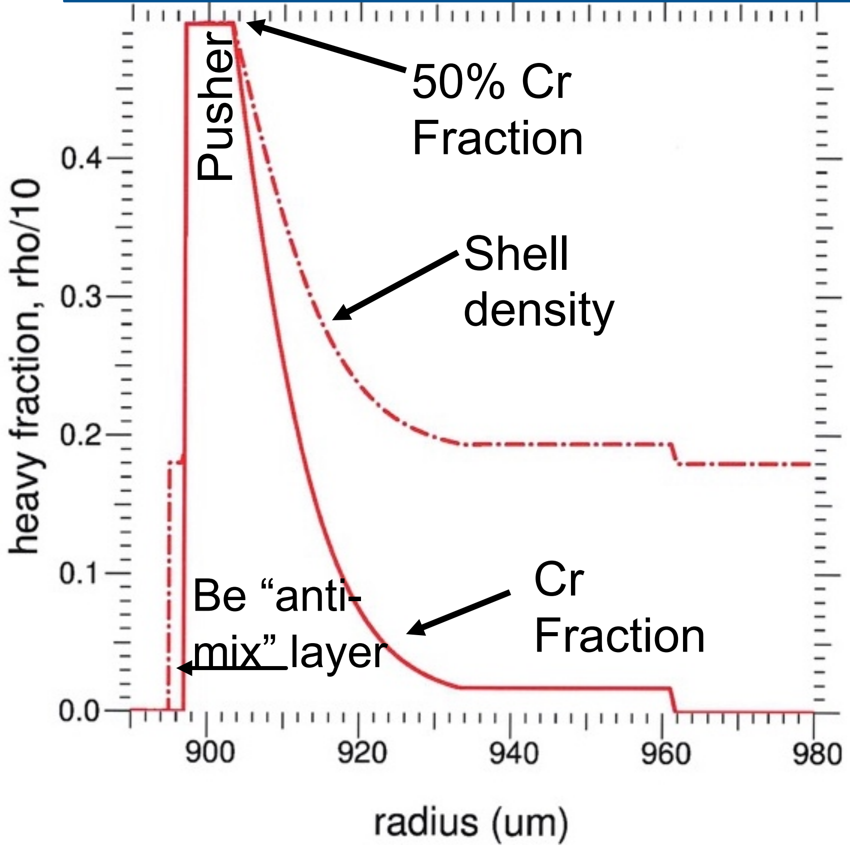

Simulated radiographs at peak velocity

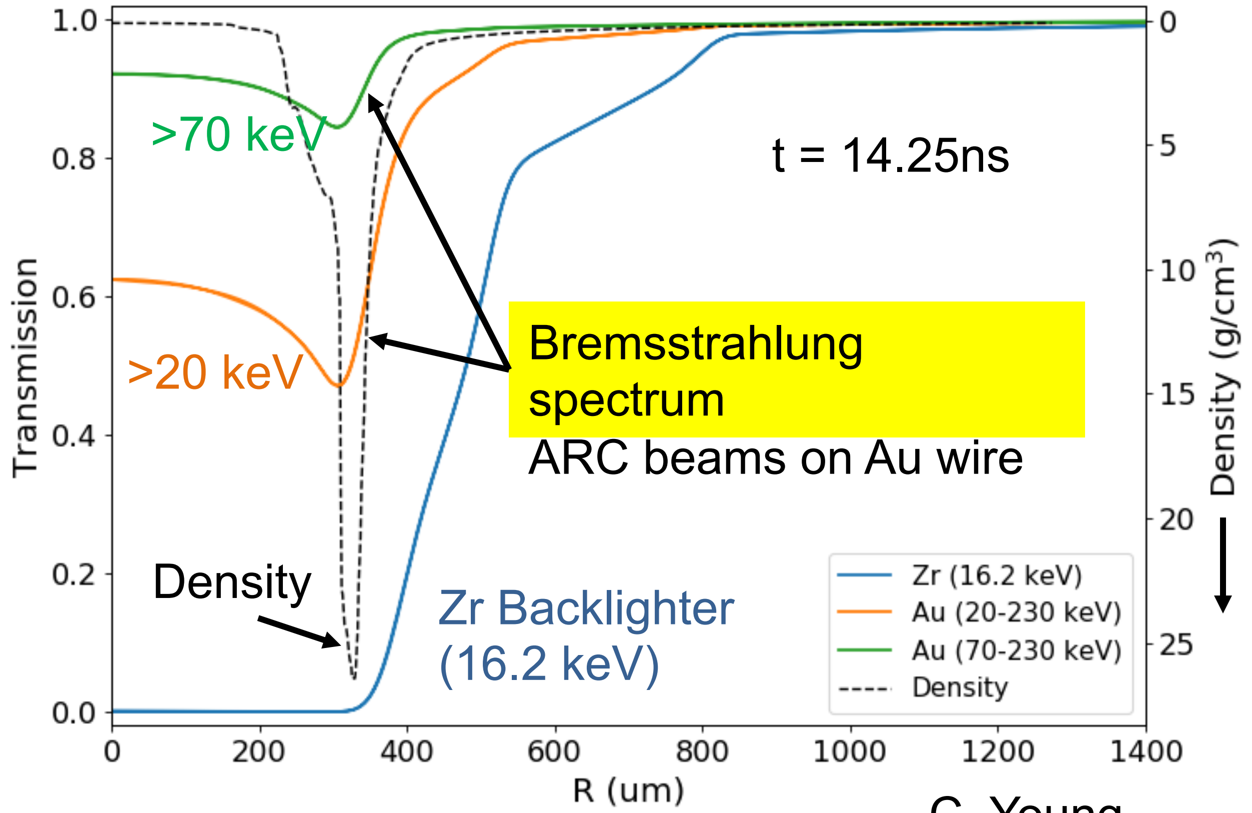

C. Young

A hard x-ray backlighter is needed to image the inflight shell

The Advanced Radiographic Capability (ARC) was used to generate the hard x-ray sources for a pair of in-flight PSS images

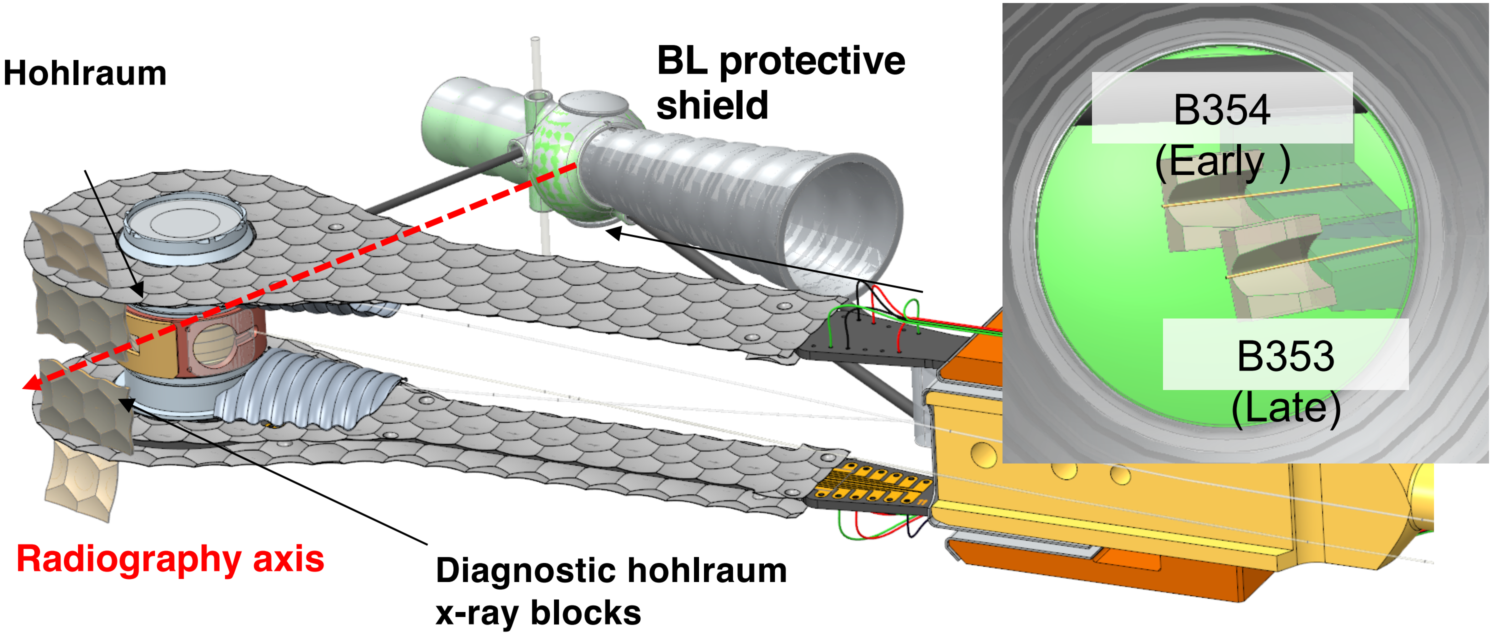

U-Flag with 25 μm Au wires backlighters

The U-Flag plasma mirror helps us capture more energy in the beamlet**

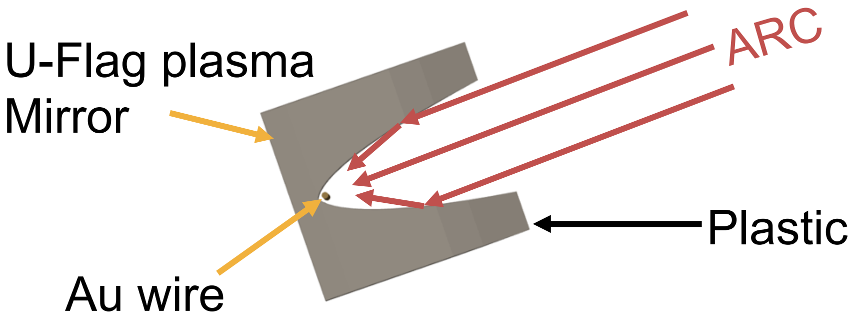

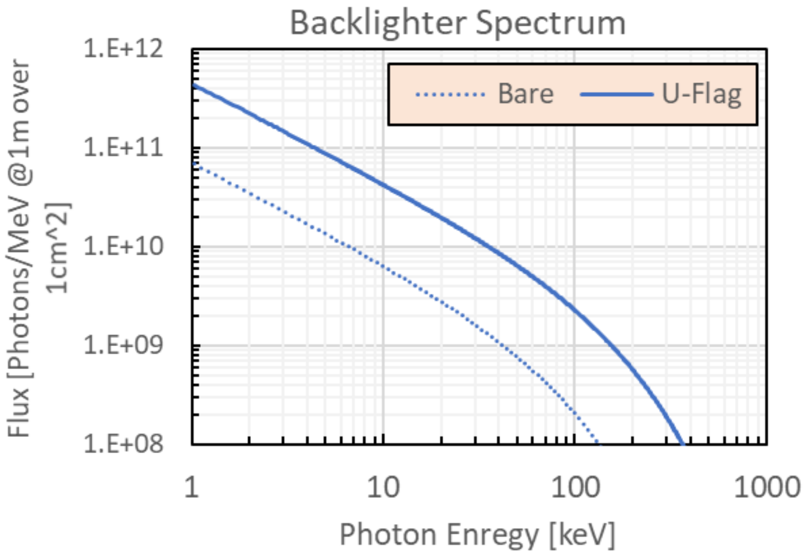

- **2 ARC beamlets per wire with 0.75kJ & 30 ps per beamlet**
- **Wires stand-off distance from capsule: 30 mm**
- **Detector distances: Image plate (600 mm), AXIS (760 mm)**
- **Magnification = 21x (IP) & 26x (AXIS).**

Tommasini et al, Phys Rev Lett **125, 155003 (2020)
A. G. MacPhee et al.,*Optica*, **7 (2), 129 (2020)

In-flight PSS image was obtained on the first attempt, but only on the first frame

Late BL (T=16.1 ns)

Early BL (T=15.4 ns)

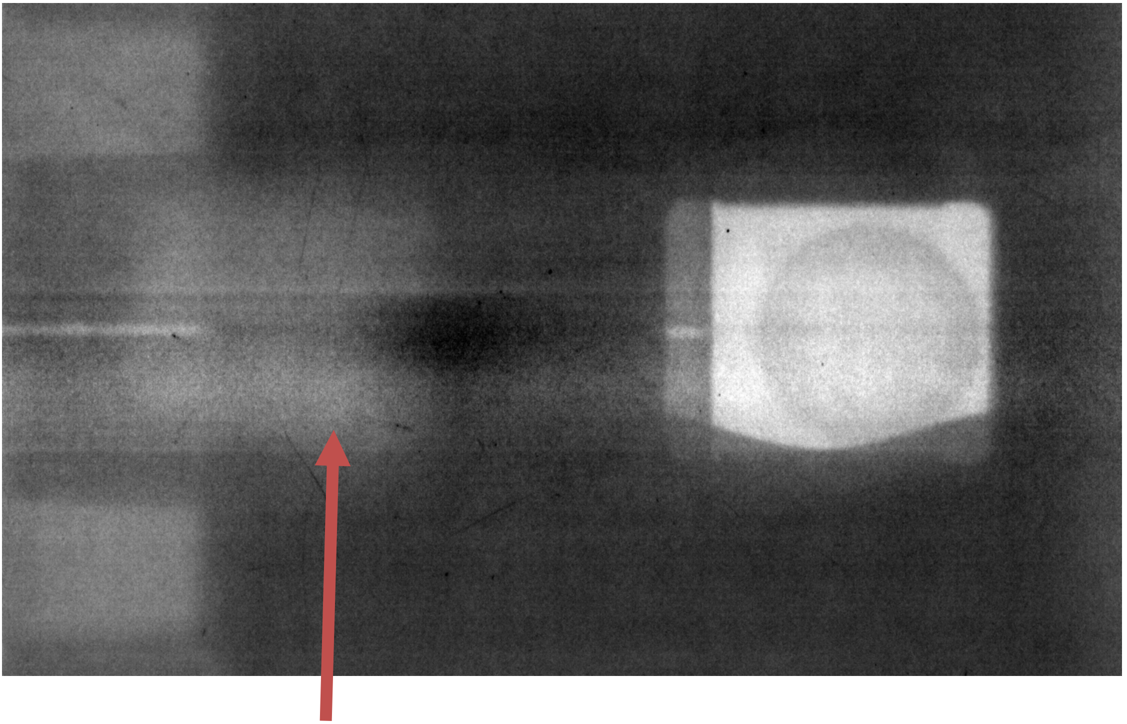

Late image lost

Early beam "splashes" onto late U-flag

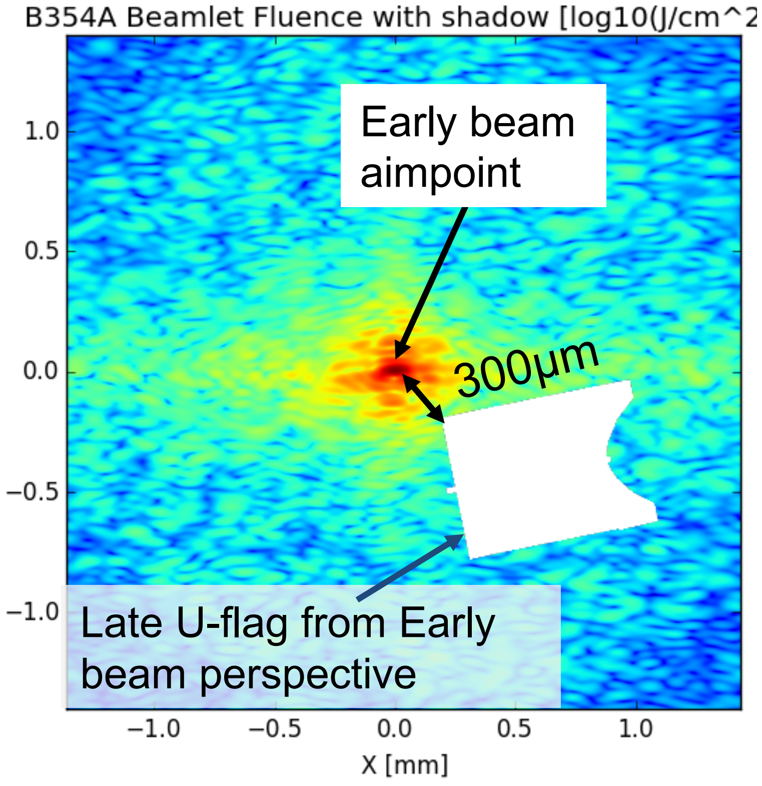

Small adjustment to position and delay is predicted to solve the issue

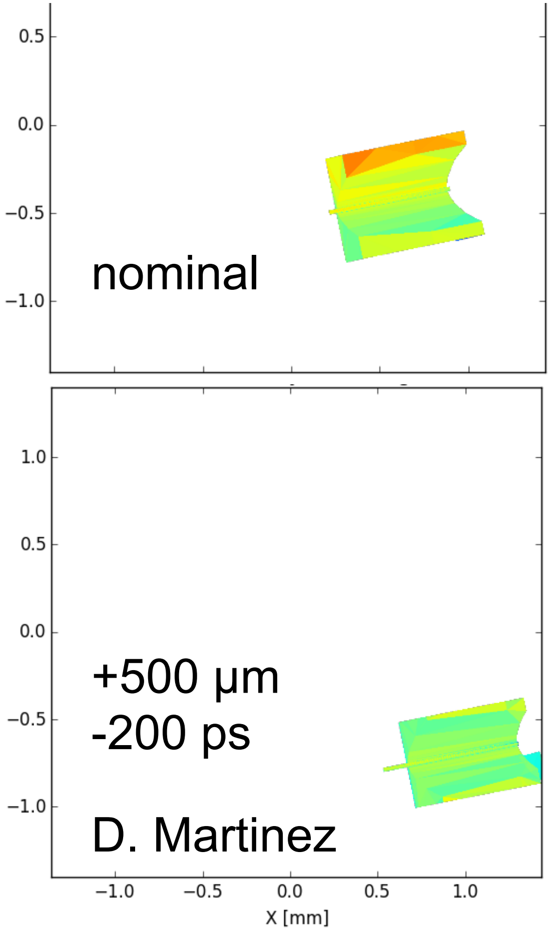

As a result, the following shots produced two successful radiographs on both AXIS and Image plate

N200510

Hohlraum bgrd.
Absent on AXIS

Image plate

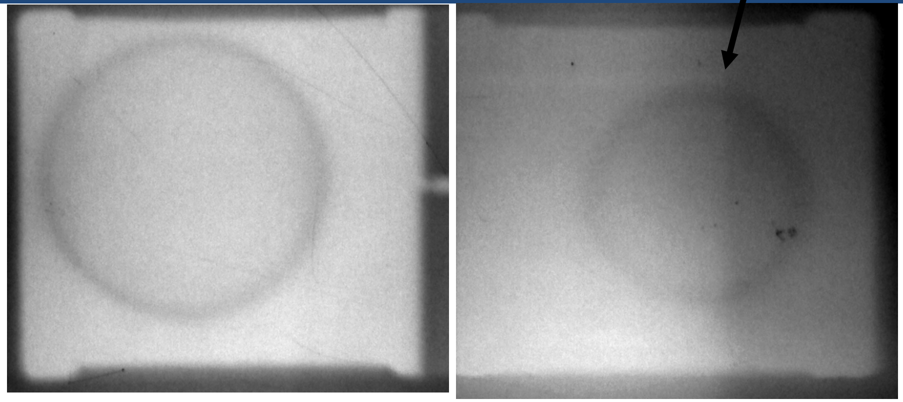

AXIS gated detector

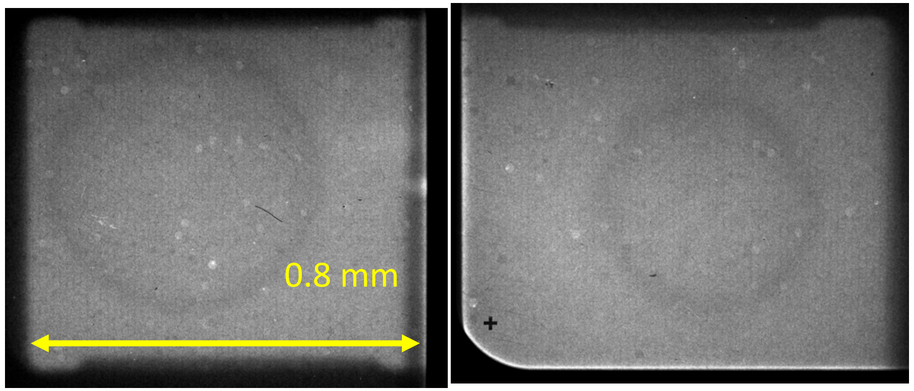

N200706 Δλ= 1Å - pancaked

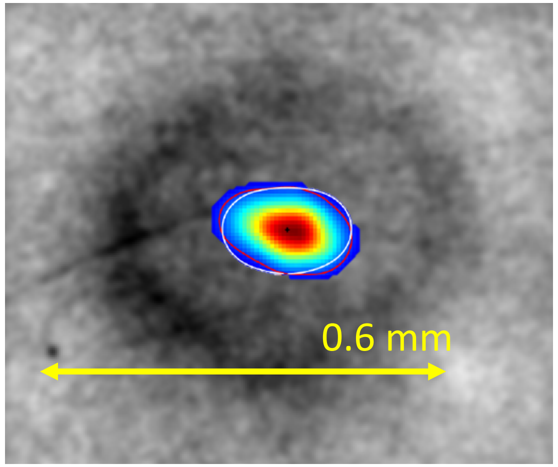

N200803 Δλ= 1.3Å - round

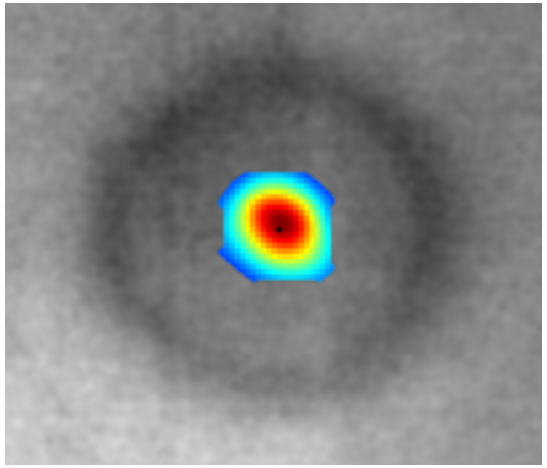

ARC combined with DD neutron images are used to assess P2 time dependence

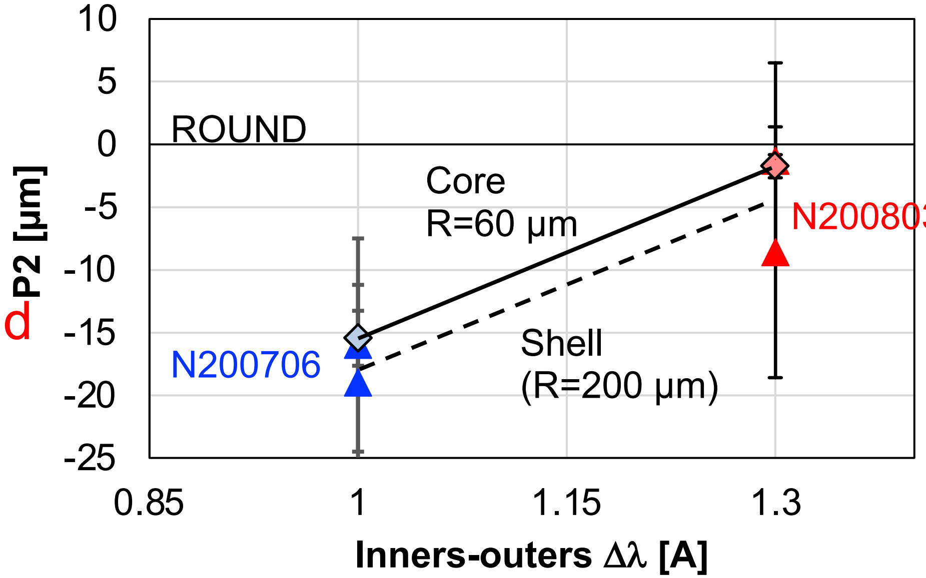

Similar shell and core P_2
(no symmetry swings)

DT Symcaps tested the Δλ "playbook" and provided a first indication of the efficacy of enhanced confinement

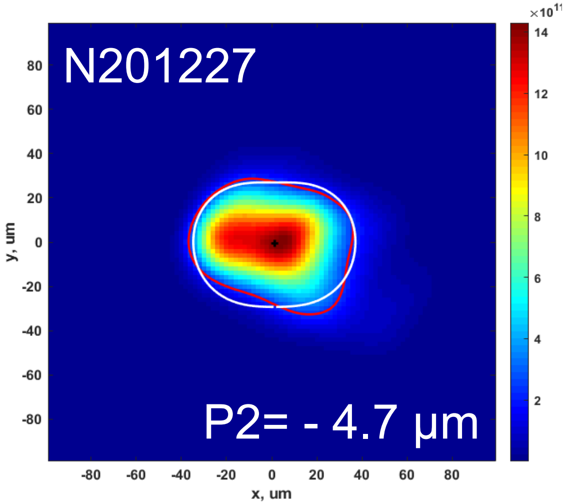

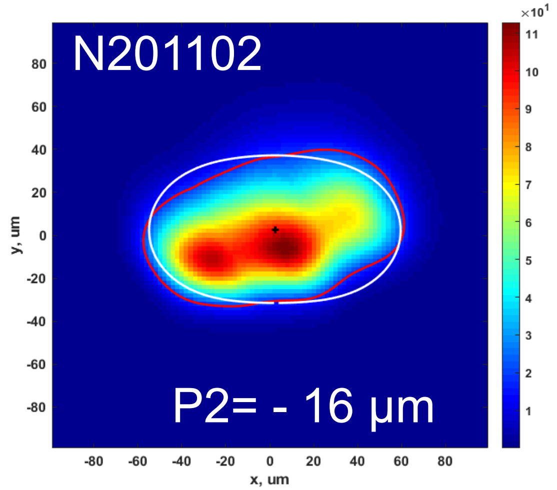

N201227 @ bang time

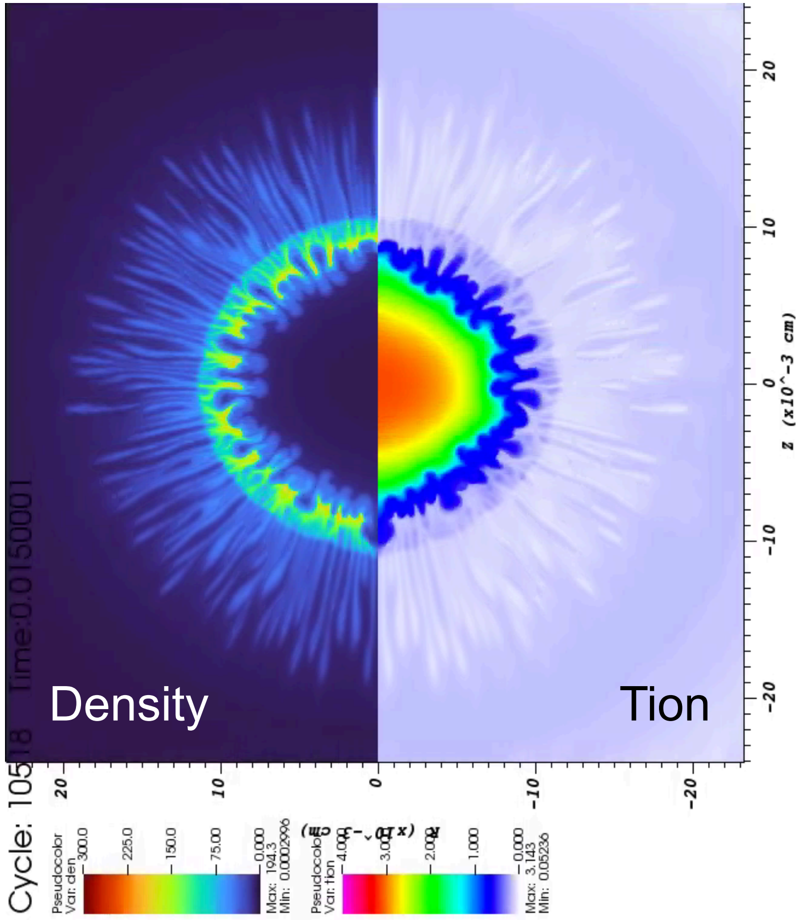

ARES – J. Pino

Comparison of PSS and low-Z symcaps of comprable size

	N201227 PSS	N200215 HDC
IR (µm)	877	844
Velocity (km/s)	250	380
T_{ion} (keV)	2.79	3.92
Yn (e14)	8.94	11.8
YOC	30%	65%

At 130 km/s lower velocity, and with more severe effects of mid-Z mix, the PSS delivers comparable performance ot the high-velocity implosion

Outline

- Theoretical description of the ignition regime
- Description of the pushered single shell (PSS) design and capsule fabrication
- PSS results on the NIF
- Detailed analysis of PSS stability

Gradient design and reduced velocity give the layered PSS the advantage over the "stable" BigFoot implosion in 1D stability

3-shock drive comparisons

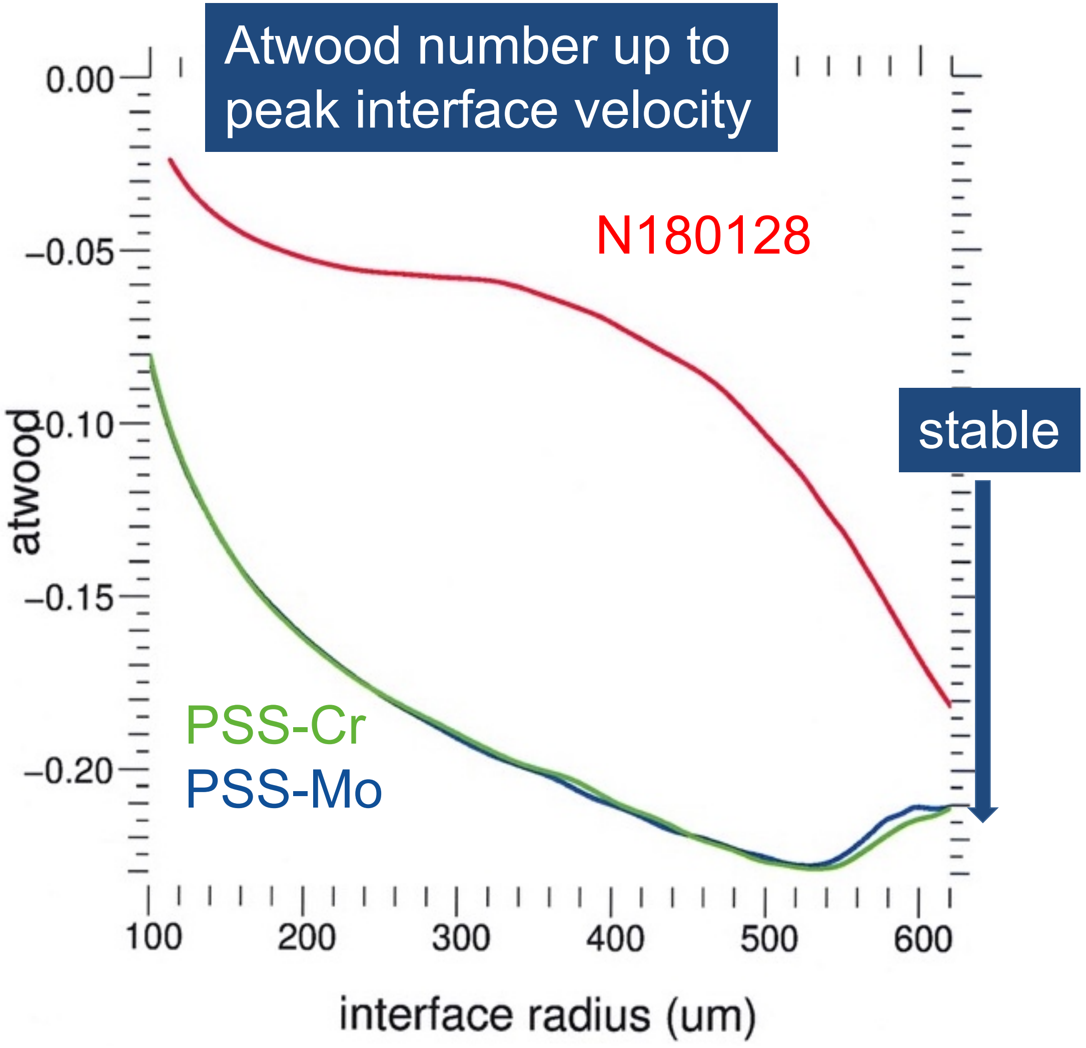

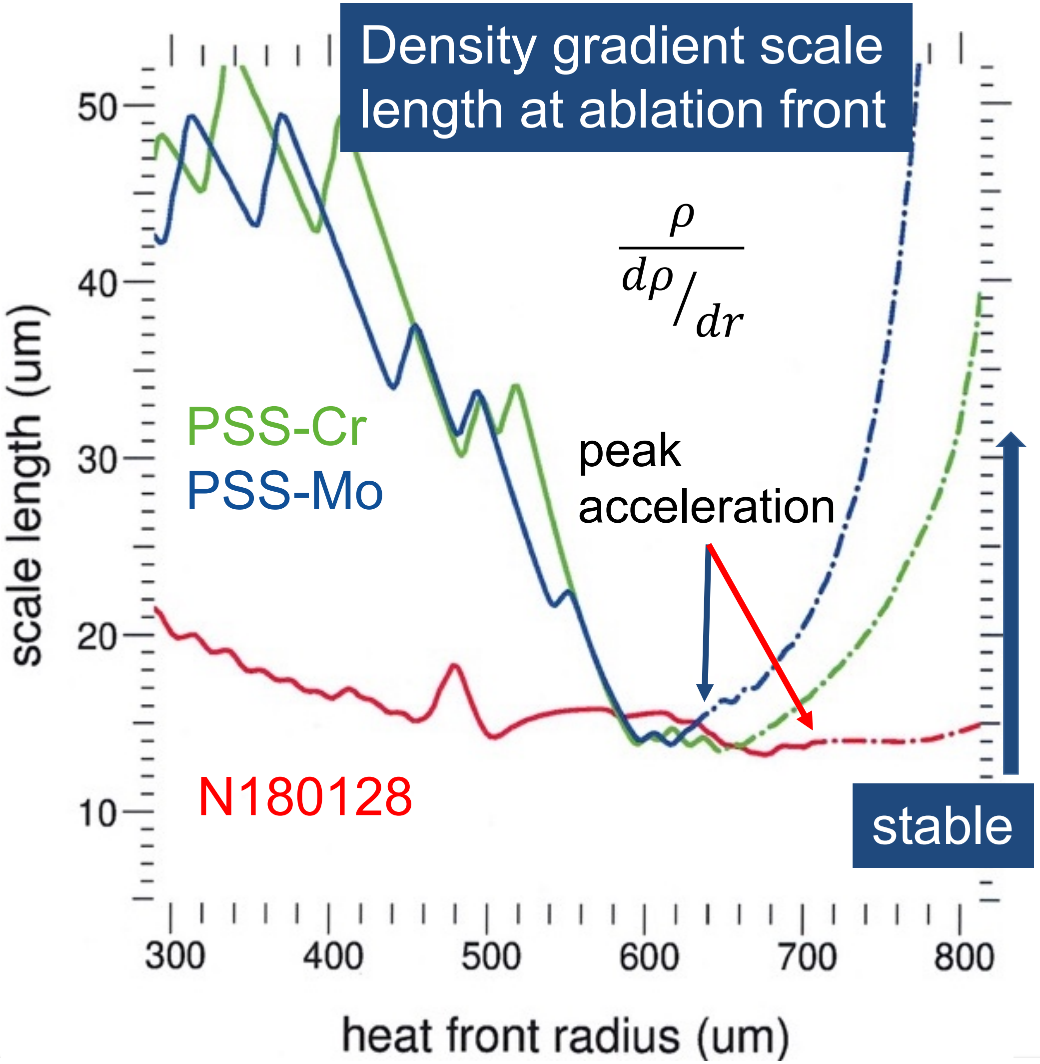

High mode capsule-only HYDRA simulations are used to evaluate linear instability growth at unstable interfaces for similar adiabat implosions

$$\gamma_k = \sqrt{\frac{gk}{1+kL}} - \beta k u_a$$

L = ablation scale length
u_a = ablation velocity

Ablation front growth factor at peak velocity

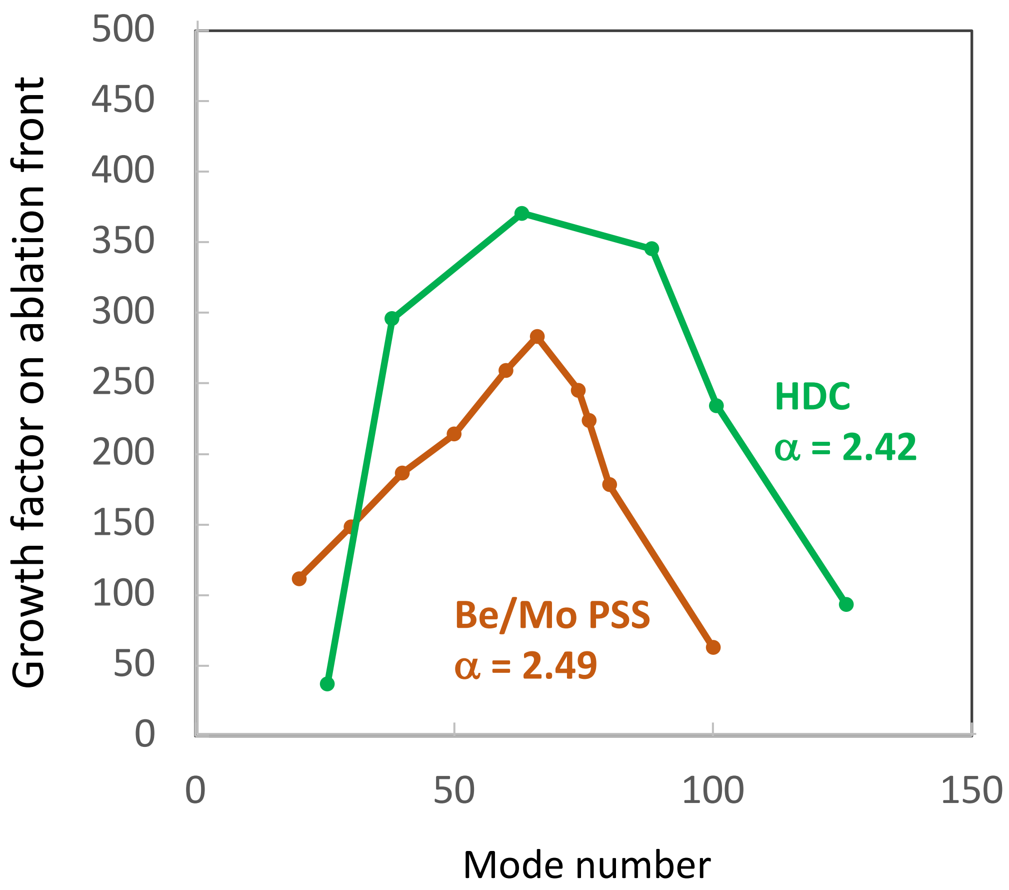

$$\gamma_k = \sqrt{Agk}$$

A = Atwood Number

Hot spot growth factor near stagnation

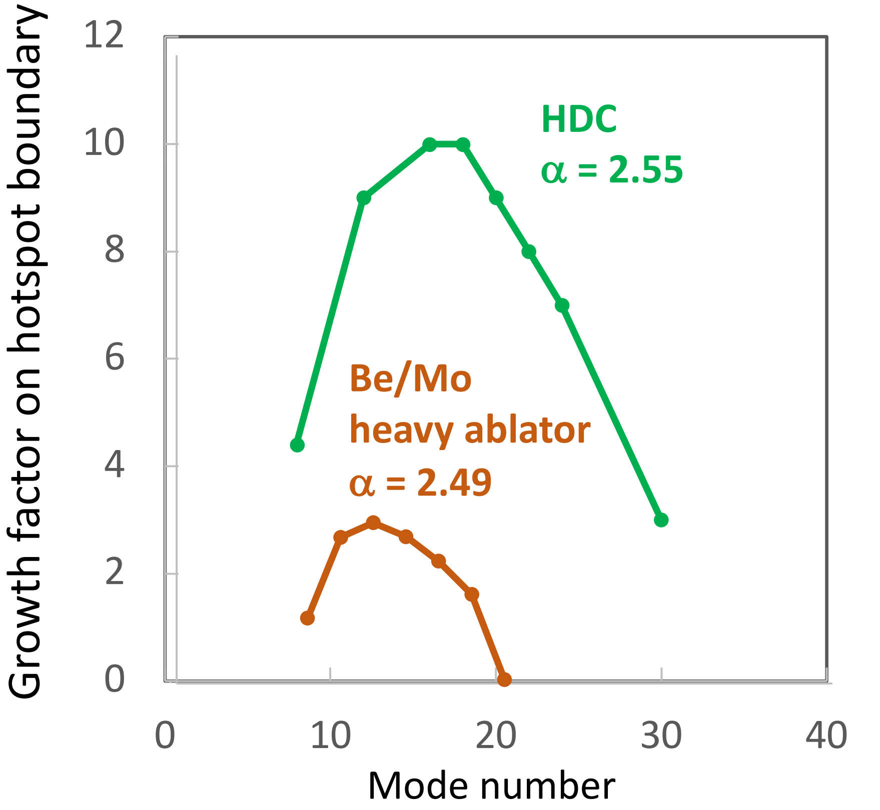

HYDRA: D. Ho

Using the measured surface roughness, high resolution capsule only simulations predict good confinement of the fuel at ignition

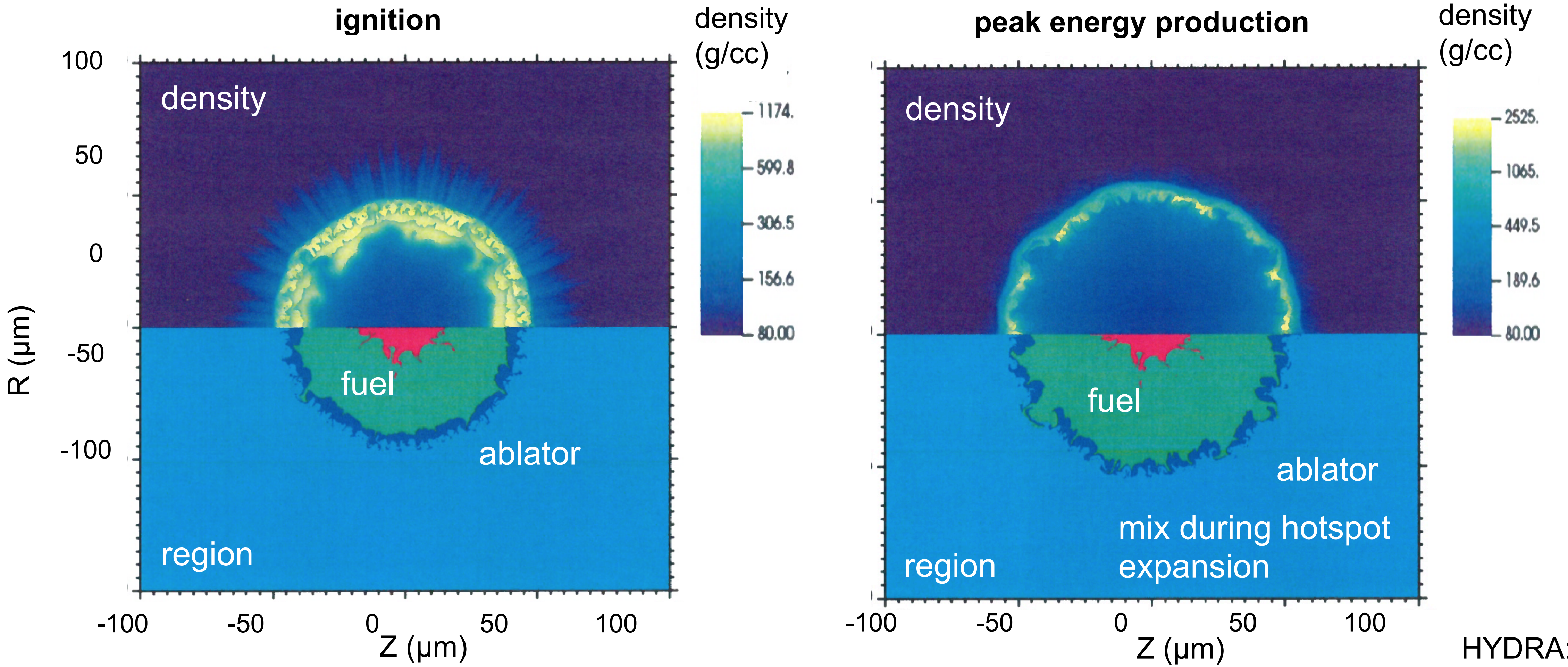

HYDRA: D. Ho

Good deceleration-stability results in an intact fuel ablator interface; the inner Be layer helps control expansion phase mix

A slower, more massive implosion, the pushered single shell (PSS) offers a fundamentally different trajectory towards the ignition threshold

- We describe a threshold that motivates the design the PSS, reaching ignition at lower velocity and temperature
- Using ARC, the ID PSS platform on NIF has demonstrated tunable long-pulse implosions of the kind necessary for low-adiabat compression
- The graded-density profile, successfully fabricated into Be capsules, predicts to mitigate ablation front instability so as to allow good compression at increased confinement

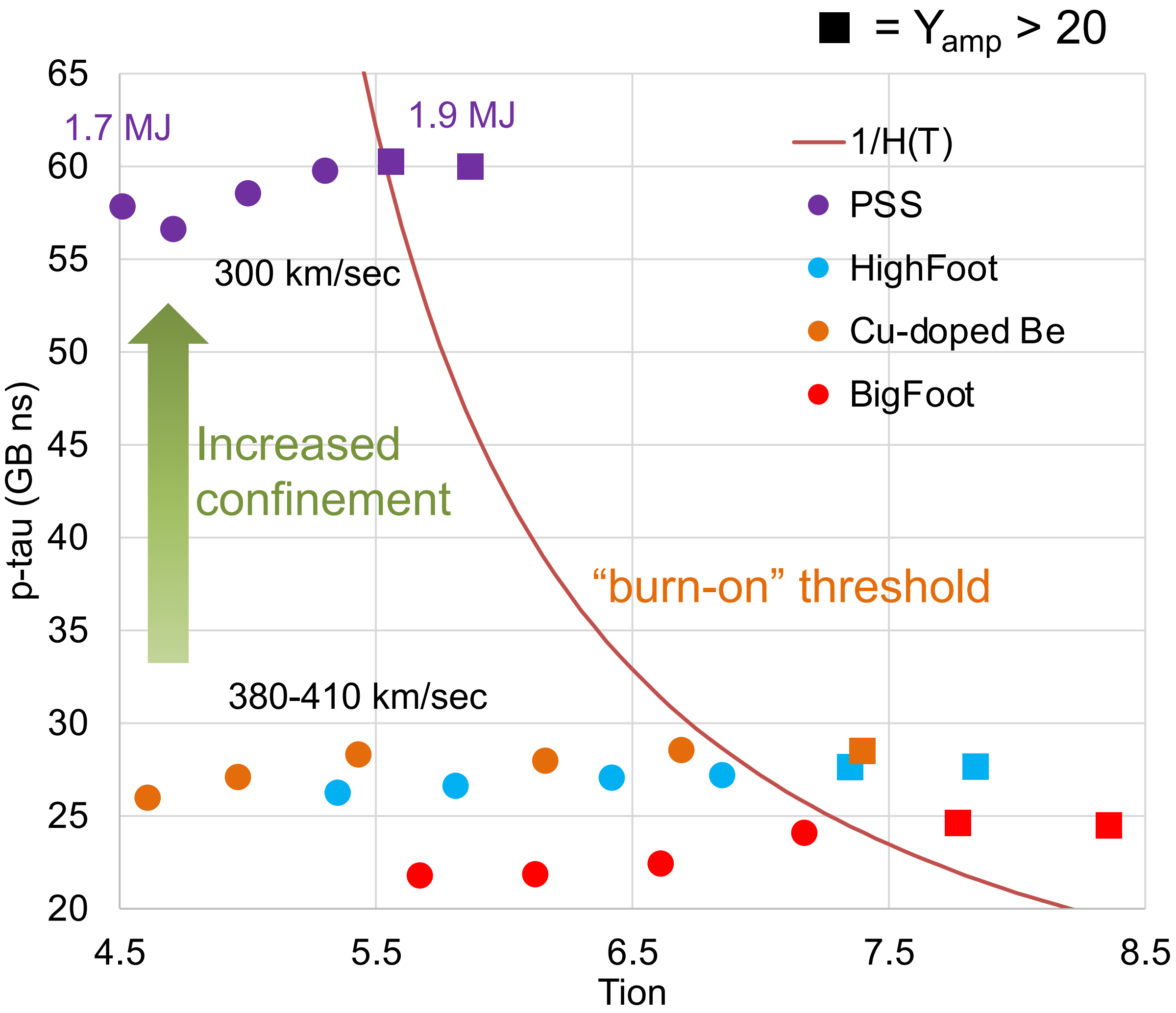

Lawrence Livermore National Laboratory